Design, Analysis and Fabrication of Secondary Structural Components for the Habitat Demonstration Unit – Deep Space Habitat

Russ Smith [1] and W. Mike Langford.[2]
NASA, Langley Research Center
Hampton, Va. 23681

In support of NASA's Habitat Demonstration Unit - Deep Space Habitat Prototype, a number of evolved structural sections were designed, fabricated, analyzed and installed in the 5 meter diameter prototype. The hardware consisted of three principal structural sections, and included the development of novel fastener insert concepts. The articles developed consisted of: 1) 1/8th of the primary flooring section, 2) an inner radius floor beam support which interfaced with, and supported (1), 3) two upper hatch section prototypes, and 4) novel insert designs for mechanical fastener attachments. Advanced manufacturing approaches were utilized in the fabrication of the components. The structural components were developed using current commercial aircraft constructions as a baseline (for both the flooring components and their associated mechanical fastener inserts). The structural sections utilized honeycomb sandwich panels. The core section consisted of 1/8th inch cell size Nomex, at 9 lbs/ft^3, and which was 0.66 inches thick. The facesheets had 3 plys each, with a thickness of 0.010 inches per ply, made from woven E-glass with epoxy reinforcement. Analysis activities consisted of both analytical models, as well as initial closed form calculations. Testing was conducted to help verify analysis model inputs, as well as to facilitate correlation between testing and analysis. Test activities consisted of both 4 point bending tests as well as compressive core crush sequences. This paper presents an overview of this activity, and discusses issues encountered during the various phases of the applied research effort, and its relevance to future space based habitats.

Nomenclature

A = area
$A_{c,fs}$ = area, core and facesheets
$L_{c,fs}$ = length, core and facesheets
E_c = modulus, effective core
E_{fs} = modulus, effective facesheets
E_{22} = modulus, thru thickness of core (same as E_c)
F = force
$G_{12,\ 23}$ = modulus, shear, ribbon and transverse directions
K_T = stiffness, effective total
K_{fs} = stiffness, face sheet
K_c = stiffness, effective core
P = pressure
δ = displacement
$\varepsilon_{t,c}$ = strain, tensile and compressive
ε_{vm} = strain, Von-Mises
$\mu\varepsilon_{t,c}$ = micro-strain, tensile and compressive
$\mu\varepsilon_{vm}$ = micro-strain, Von-Mises
$\sigma_{t,c}$ = stress, tensile and compressive
$\sigma_{c,ult}$ = stress, ultimate compressive
ρ_c = density, core
ν_{ij} = Poisson's ratio, principle directions

[1] Senior Research Engineer, Structural Mechanics and Concepts Branch, RD, MS 190.
[2] Senior Design Engineer, Aeronautics Systems Engineering Branch, ED, MS 238.

I. Introduction

The Habitat Demonstration Unit - Deep Space Habitat (HDU-DSH) (Fig. 1) is a demonstration precursor prototype with a principal focus on ergonomic and human factors effects, but with continued associated structural development. Structural development (or evolution), includes such sections as floors, floor support beams, hatches, doors, airlocks and egress/ingress porches, access ways, as well as numerous other critical systems[1]. The initial HDU-DSH prototype was designed and fabricated at the Langley Research Center (LaRC) and consists of eight pie type sections, as can be seen around the upper hatch section in Fig 1. The initial prototype was referred to as Generation 1, or Gen 1, with the efforts outlined in this report being part of the Generation 2, or Gen2, prototype. This paper focuses specifically on evolved secondary structural components[2] associated with Gen2. The pie shaped cylindrical sections alternate between ingress/egress areas, and specific work areas such as Geo-Lab, medical operations, general maintenance, and so on (Fig. 2). Between each of the pie shaped sections of the HDU-DSH, are radially oriented steel bulkheads[3], to which the outer shell wall sections are joined. Although the initial HDU-DSH (i.e. Gen1) was not designed as a pressure vessel, a final DSH prototype design with advanced primary structure, would carry pressure loads along with an associated factor of safety[4]. The applied research reported here, comprises one of many possible solutions for DSH type structures, which will have to be as mass efficient as possible, while also being qualified over long periods of time (between 5 to 15 years).

Specific HDU-DSH structural sections targeted for advanced development were: 1) $1/8^{th}$ of the primary flooring section (section "A"), 2) the upper hatch area, and 3) a primary inner radius floor beam support. Figure 1 shows both the upper hatch section as well as section A via an external view. The specific main flooring area is called out in Fig. 2 (with the flooring section removed) in order to show the inner radius support beam. These sections were specifically targeted because of their relevance to habitats in general[2] and the fact that primary shell structure development did not fit within the current program guide-lines.

There are numerous goals associated with the development of these sections. These goals include design and fabrication approaches, analysis methodologies, and testing regimes to allow for confidence in correlation between material properties, and associated analysis results. However, given the rapid prototyping focus of the HDU-DSH, the primary focus was on the design and fabrication specifics, as well as the integration of these sections, into the prototype. Analysis and testing were conducted to the greatest extent possible in a very compressed time frame. It was particularly important to go from the current structural sections in the HDU-DSH, to structural sections which are of relevance to an actual space habitat and which could be flight qualified. The sandwich construction selected for this study also has the ability to be multi-functional, and will potentially dove-tail into such activities as radiation shelters. This paper will outline a number of these issues and their potential relevance to an actual space habitat.

II. Design and Fabrication Details

The mass efficient sandwich composites installed in the Boeing 787 Dreamliner were used as a reference baseline for evolving the structural elements to be integrated into the HDU-DSH. Additionally, due to its large implementation of sandwich components, the Airbus 340 also provides a reference point for structural inclusions, attachment methods, and repair approaches[5].

All of the sandwich components utilized style 7581 woven E-glass cloth with ECG 75-1/0 rovings, with an 8 harness satin weave. The cloth was 9 oz. per square yard with a nominal pre-preg epoxy content of 37%. Facesheets consisted of 3 ply, 0.010 inch per ply, for a total facesheet thickness of 0.030 inches. The honeycomb core consisted of $1/8^{th}$ inch cell size Nomex, at 9 lbs/ft^3 and was impregnated with a phenolic resin system. Due to previous 1^{st} generation HDU construction constraints, it was required that the advanced structural panels be stacked, such that a total panel segment height of 1.44 inches (nominally) was obtained. Figure 1 shows both the upper hatch section as well as section A via an external view. The specific main flooring area is called out in Fig. 2 (with the flooring section removed) in order to denote the inner radius support beam section.

The 4ft by 12ft panels were received as part of a six panel set and were manufactured by the M.C. Gill Corporation which has a long history of aircraft grade sandwich panel constructions. All of the panels were rough-cut utilizing water jetting technology. Bonding of the back-to-back sections was accomplished via Hysol 9359.3 structural adhesive and the perimeter edge reinforcement was accomplished utilizing a filler compound. All of the edge sections of the honeycomb composite were nominally cored out, in roughly a semi-circle due to the core adhesive, to a mid-span depth of about $3/8^{th}$ of an inch. Due to the use of the water jetting fabrication approach, a

mild “scalloping” on the back side composite facesheet was produced. In the case of this fabrication effort, such effects were negligible. For more precision pieces, which would be required for flight qualified articles, either the water jetting technique would need to be modified, or a more refined cutting technique would need to be used (i.e. precision sawing with either a carbide, or diamond tipped type fine blade). However, water jetting of the major sections proved acceptable.

In addition to the evolved secondary structural sections which were developed as part of this applied design and research effort, a series of advanced insert prototypes, for mechanical fastener tie down, were developed and evaluated, prior to the final inserts designs. The inserts were auto-fabricated utilizing acrylonitrile butadiene styrene (ABS) M30 grade engineering material in a fused deposition production machine. To help fast track evolved sections towards flight certification, Federal Aviation Administration (FAA) approved 10-32UNF cap screw fasteners were used in all of the flooring tie down locations, and wherever else possible. All of the sandwich sections developed were done so based upon a 50 lbs/ft^2 live load with an associated Factor of Safety (FS) = 1.5.

A. Primary Flooring Section

Shown in Fig. 3 is a VectorWorks (VW) 2010 CAD model rendition of the primary flooring section A as previously mentioned. The exploded view shows the upper level, inner and outer flooring sections, as well as the mating sub floor areas. There is a nominal 1 inch indexing between the upper sections and the sub floors to allow edge pick-up with the inner mold line (IML) of the interior shell section of the HDU-DSH. The staggering of these sections also allows for better load pick up, and stability of these sections, as tied down to the floor support beams. The access hatch follows a similar design approach, and has a 1 inch perimeter lip upon which it rests when in the flush condition. It is designed to be readily removed for easy access to avionics racks, and other internal component hardware, which are beneath the primary flooring.

Shown in Fig. 4 are some of the initial fabrication details of the floor as well as a final picture of the flooring section prior to shipment to JSC for installation. Water jetting of the sections had occurred previously to generate the specific sections. Shown in Fig. 4c is the final installed flooring section within the HDU-DSH. The inner radius floor beam support is not shown due to the fact that the primary flooring is covering it.

Similar issues will be encountered for actual flight qualified structure, although design requirements could be vastly different. More precisely, the same types of fabrication issues, core edge re-enforcements, adhesive type selection, mechanical fastener inserts and tie down issues, and so on, will also need to be addressed. For instance, in the case of this development effort a 1g gravity environment was a design driver. Specific mission locations may have no gravity, or very small gravity loads, to about 0.38g (i.e. Lagrange Points (LP), Near Earth Asteroids (NEAs), Lunar and Martian environments). However, gravity loadings are not the only load requirements. Flight qualified hardware will also need to be certified for launch loads, potential vacuum environments, and possibly extreme thermal conditions (both cryogenic and elevated). In all load cases, both the primary and secondary structure will have similar design, fabrication, testing, and analysis issues and will require proper material properties characterization.

B. Inner Radius Beam Floor Support

The spacing between floor support beams was a nominal 20 inches on center, with the inner radius floor beam (FB) section picking up an additional edge support at the interface with the interior ring flange of the central internal core of the HDU-DSH (i.e. the cyan colored area in section A of Fig. 2). The nominal lengths of the support beams, proceeding radially outward, at the mid span web location, were 30.84 inches, 46.18 inches and 61.50 inches respectively. The specific floor beam replaced for this effort was the inner radius beam with a span of 30.84 inches. Shown in Fig. 5 are the specifics of the sandwich inner radius beam. The flange widths were nominally 6.00 inches top and bottom.

Shown in Fig. 6, are the brackets that were designed to interface with the existing steel bulkhead structure of the HDU-DSH. They interfaced directly with the lower flange to bracket inserts as shown in Fig. 5c. The bulkhead sections were designated as A on one side and B on the other, and hence each two bulkheads would come together at each of the 1/8th pie sections to form an A/B pair. The steel bulkheads to inner radius floor beam brackets were constructed from 5/16 inch thick, grade 50, A-572 steel and had the upper tangs welded to the individual bracket assemblies.

Note that the specific location of the inner radius floor support beam is shown in Fig. 2. Additionally, the lower flange outer edges of the floor beam had to be cut, in-situ, during installation into the prototype, to allow for proper seating into the radius areas of the bulkhead brackets (Fig. 6). As outlined in the design and fabrication detail section, similar mechanical fastener insert components will be relevant to actual flight level floor beam supports as well.

C. Upper Hatches

The final evolved secondary structural components investigated consisted of two types of hatches where the work platform (i.e. an elevator to the second story) of the HDU-DSH, interfaces with the upper loft section (Fig. 1). Shown in Fig. 7 is the initial structural hatch concept, based predominately on the Gen 1 design. The initial prototype design had the rib stiffening elements run uniformly out towards the perimeter of the lower, bottom most, panel section. The as constructed, upper hatch concept #1 structural panel is shown in Fig. 8. Note that the stiffening ribs alternate between long and short and that inserts were required to facilitate handle attachment. The handles had a torsional spring feature which would automatically return them flush with the surface. There was also a relatively soft rubber section on the handle in order to reduce any potential dinging of the upper surface panel facesheet.

Due to concerns about the potential weight of the upper hatch section, affecting the ability of smaller crew and service personnel to be able to easily lift the hatch off of the work platform during an emergency, as well as routine ingress/egress operations, an additional hatch concept #2 was developed and fabricated. This weight concern was addressed by using only a single sandwich layer, and did not include the rib stiffening elements associated with concept #1. It should be noted that the design space requirements shifted frequently, with an initial idea of the hatch being flush with the surface and a primary load bearing type hatch (i.e. concept #1) which would be opened via a mechanism interface with the elevator. There is a railing system on both the 1st floor and 2nd story loft section (which is not shown in Fig. 1), which is intended as a safety feature. The railing precludes crew, or other personnel, from stepping on the hatch when the work platform is positioned in the 1st floor section. The specifics of the upper hatch concept #2 and it's installation are shown in Fig. 9. It should be noted that hatch concept #2 was constructed using only a single layer of sandwich board and mounted directly to the four, nominally 2 inch diameter tubing, which forms the upper part of the elevator. The flange leg interface, shown in Fig.9e, allowed hatch concept #2 to slide directly into the open tubing section of the elevator. Hatch concept #2 was acceptable because the loading requirements changed from a load bearing structure, to one in which personnel would not be allowed to stand on the hatch (even though one of the authors can be seen proof loading concept #2 in Fig. 9d.) This shows just how stiff a single layer of the sandwich construction actually is, with a nominal load in Fig. 9d of about 300lbs.

Impacts to actual flight type hardware, particularly with respect to handle sections, will be very similar. Methods will have to be developed which allow for flush with surface, and self retracting type handles (as design requirements dictate). Additional recessing of attachment locations, such as those shown in Fig. 9b, will also need to be addressed for flight level hardware.

D. Inserts Development & Evolution

Specialized hardware was also developed to allow for the incorporation of the evolved HDU-DSH secondary structural elements. An example of the custom hardware includes such items as ABS inserts for the flooring section and inner radius floor beam. Drawing from the aircraft industry with respect to attachment of such sections, three categories of insert concepts were developed: 1) flush with the surface[6] 2) beveled edges, with minimal protrusion above the surface, and 3) proud (or protruding) inserts. Shown in Figs. 10 thru Figs. 12 are all of the outlined insert types. The flush with surface prototype (Fig. 10) was discarded early in the prototyping cycle due to its localized crushing of the composite facesheet. However, both of the beveled edge and proud insert concept types were retained, and evolved for subsequent integration.

All of the initial insert concepts were based upon a two part, or multi-part design (Fig. 13). There was a component which mounted from the top surface, and a mating component which was attached thru the bottom surface, as well as intermediate pieces (Figs. 13a-b). Insert concepts for the floor beam were always limited to two pieces initially, because they only had to penetrate a single sandwich layer. Due to the unique nature of the flooring, and beam configurations, there were no commercial off the shelf (or COTS) component parts available. Schedule, and costing associated with the acquisition of appropriately designed, and commercially derived fasteners were prohibitive. This required that the rapid prototyping and design effort be initiated. Typical commercial inserts are either machined from metallic stock (generally aluminum), or from high end engineering thermoset systems, such as Turlon. Due to

the machining required, and post machining operations such as de-burring, buffing, and other final detail work, a more efficient, and simpler manufacturing method was desired.

There was a necessity to see the flooring sections, particularly in the event of a power outage, or lighting loss, for emergency ingress/egress purposes. A similarly configured insert concept, but which was manufactured from Glow in the Dark (GitD) material, is shown in Figure 14. However, the material wasn't as robust as the ABS, and fabrication was accomplished in a more traditional lithography process which had a much lower density resolution than the ABS M30 type inserts.

After numerous trials, and fabrication concepts, the final, novel, insert designs are shown in Fig. 15. The final designs account for the loading of the primary flooring section, the flooring support beam, and allow for sandwich sections of various thicknesses. The final insert configurations were chosen for a number of reasons; ease of fabrication, installation, minimization of rework (i.e. post machining type issues) and adhesive clean up. They also allowed for maximum honeycomb core retention but with significant adhesion to the core. Utilizing the fused deposition manufacturing approach, the inserts developed in this activity are lighter, require no machining or secondary processing, and have less adhesive mass than similar state-of-the-art aviation inserts. They also allow for greater core retention, due to reduced core out of the core section itself during hole drilling, and promote weight savings which are critical for space habitats. The inserts can be geometrically tailored to fit almost any space relevant requirement, and in conjunction with the sandwich board construction, form one of the leading structural approaches of future space habitats[2].

III. Testing in Support of Evolved Components

Test sequences were devised to determine primary analysis model input values. In order to determine values for analysis input, a 4 point bending test was developed, based primarily upon ASTM D7249[7] and ASTM C393, as well as a compression test. Typically, the facesheet modulii, and strength, are the most important material properties for such sandwich type constructions, but the core must be accurately accounted for as well. A typical approach is to model the core as a 3D orthotropic solid with strengths experimental determined[8] . The referenced approach was discovered after testing had been completed, but should be used in future efforts. Honeycomb cores have effective values that are of great importance. The two shear modulus values, G_{12} and G_{23}, as well as the effective compressive core modulus value, E_c (or more typically E_{22}). These modulus values, along with their associated Poisson's Ratios, v_{ij}, are required for an engineering mechanics approach to model the core. The compressive core test method was developed in order to determine the effective thru the thickness modulus, E_c. The tests also helped to verify the facesheet strength values, which vary in tension and compression, as well as the facesheet modulii. More precise characterization will improve the development of optimized sections of this type of structural concept for future structures. The facesheets were qusi-isotropic, in plane, as supplied by the vendor.

A. 4 Point Bending Tests & Results

Shown in Fig. 16 is a 4 pt bend testing fixture in order to determine material properties for model development. The 4 pt bending tests were conducted to determine the facesheet modulus, and its associated strength. The loading set-up consisted of the following: 1-inch radius steel load introduction bars at a major span of 10 inches and a minor span of 5 inches. Each of the load bars had Shore A Brinnell hardness 60 rubber pads which were used to minimize localized facesheet failures during testing. Data recording was set at a rate of 4Hz, and both pre-zeroing, zeroed data and the entire load sequence, including a return to zero displacement, were recorded throughout all tested specimens.

Figure 17 shows a typical failure mode, and location, and also shows the ribbon and transverse directions. Failure did not occur at the load introduction points. The effective facesheet modulus was determined in accordance with ASTM D7249. Results from the verifying 4 point bend testing sequence tended to affirm the facesheet modulus (as supplied by the vendor), and also determined values for other facesheet properties. In Appendix section A the compressive and tensile responses are detailed and failure did not occur at the load introduction points.

Data shown in Table 1, is a summary of tests in both the "L", or ribbon direction, , and the "W," or transverse direction, of the core respectively. Typically, the ribbon direction of the core is the stiffest, and in general produces a stiffer facesheet stress response. In order to be conservative in assessing the structural response of the specimens, the lowest facesheet modulus was used in the updated analysis models. The specific analyses conducted are outlined in subsequent sections. The facesheet planar modulus of elasticity provided by the vendor was 2.5Msi (based upon a

polyester matrix with the same cloth type), however, 2.4Msi determined from testing was used for analytical runs. Of additional interest is the fact that the strain symmetry between the tensile and compressive facesheets is apparent in the 1000 micro-strain ($\mu\varepsilon_{t,c}$) range. However, at 3000$\mu\varepsilon_{t,c}$, asymmetries between the upper and lower facesheet strains are evident. This is due to symmetric linear behavior initially (small displacements, small rotations). The non-linear response effects of the core, and larger displacements, manifest at the higher strain levels, particularly in bending.

B. Core Crush Testing Development and Results

Shown in Fig. 18 is a representative picture of the core crush testing apparatus used to determine specific material properties, and more specifically, the E_{22}, or E_c, thru the thickness modulus of the core. The core crush specimens had A = 9in^2, with L_c = 0.66 inches and the L_{fs} = .030 inches. And were 3 inches by 3 inches wide. The single layer sandwich specimens were compressed between two flat and parallel load platens. A typical core crush test response data set is shown in Figure 31.

A spring in series formulation was constructed in order to facilitate the determination of the effective honeycomb core modulus, E_c (or E_{22}) in the thru the thickness direction as shown in Fig. 19. Therefore:

$$\frac{1}{K_T} = \frac{2}{K_{fs}} + \frac{1}{K_c} \tag{1}$$

The core crush test showed that the modulus of the total stack = 122E3psi. Accounting for the stiffness of the facesheet sections this then determines a nominal thru the thickness core modulus, E_c (or E_{22}) = 88E3 psi. This value is typical of core materials of this type of construction. The vendor supplied strength, Table 2, for stabilized compression was $\sigma_{c,ult}$ = 2,133psi. However, the largest average $\sigma_{c,ult}$ developed during the core crush test was $\sigma_{c,ult}$ = 1,939psi and represents a reduced strength value of 10% from that supplied by the vendor. This is most likely due to the larger core height of 0.66 inches vs. the 0.500 reference core height. The shear moduli , in the ribbon (L) and transverse direction (W) values (i.e. G_{12} and G_{23}) were retained as outlined in Table 2. The Poisson's Ratio values, ν_{ij} were unaffected.

IV. Analytical Results

Both the 4-pt bending test results, as well as the core crush results, were intended to be used in the refined formulation for the final analyses utilizing the analysis code of MSC Nastran[9] as well as the pre & post processor Patran[10]. A series of modeling "patch" tests were done for each of the test sequences conducted and those analysis model results were compared to test results for correlation. A patch test is essentially an analytical experiment, whereby different analytical methods are tried, such as nodal point loading, versus, distributed pressure loading (e.g. the core crush patch tests) and the differences in response noted. The patch tests, particularly for the core, were intended to show different approaches to achieving a desired response. An initial closed form analysis of the flooring section, based upon a ρ_c = 3 lbs/ft^3 is outlined in the Appendix A section and shows very low bending loads with a $\sigma_{t,c}$ = 343psi.

A. Core Crush Analyses/Patch Test Models

The facesheets in this case were modeled as solid elements, as were the core elements. Facesheet elements had one element each thru the thickness and the core had four. The X direction corresponds to the ribbon direction of the core and the Z direction corresponds to the transverse direction. Applying a uniform pressure load across the upper surface (i.e. 9000lbs/9in^2, thus, P = 1000 psi), as shown in Fig. 20, yielded a total displacement in the thru the thickness direction, or –Y, of δ = -0.0077 inches (virtually identical to test results).

The boundary conditions (BCs) imposed on the core crush patch model consisted of a six degree of freedom (DOF) fixing of the bottom most corner node, then progressing out from that corner node, in the X, Y and Z directions respectively, and allowing those co-linear nodes to move in only those directions. Additionally, all of the bottom planar nodes were confined against motion in the Y, or vertical direction (essentially simulating the very stiff bottom load platen). There were other BCs which were tried, but which didn't match up with simple analytical theory. The above BCs were verified by imposing them, then using an all aluminum material total stack (i.e. the facesheets and

the core were given basic aluminum material properties), and then checking the displacements, strains and stresses against simple theory, with an exact match the result.

B. 4-Point Bending Test Patch Models

The boundary conditions imposed on the 4-point bending patch test were that the center plane of the middle of the model was free to move only in Y, or the vertical direction only (simulating symmetric bending), as well as the bottom most, center line of rubber pad nodes being fixed against displacements. Where the rubber pads interfaced with the facesheets, those nodes were equivalenced. This approach allowed for the accurate capturing of the rubber pads effect on the model's response. This approach was again verified utilizing an elementary model which was made from aluminum only, and then checked against theory.

Shown in Fig. 21 is a simulation of the 4-point bending experiment. The total top surface load applied was F = 450lbs and which was divided between the two upper load bars. The total mid-span displacement, in the -Y, or vertical direction in the analytical model is less than that achieved during testing, δ = -.109 inches vs. δ = -0.156. The amount of displacement may have depended greatly upon the reaction of the rubber load introduction pads, as proofed by initial aluminum plate tests. It was a linear analysis of a non-linear response. Next, as shown in Fig. 22, the same model sequence was conducted but was done as a non-linear analysis, which allowed for large displacements as well as follower forces. Of great consequence is the fact that the test results for the mid-span displacement, yielded δ = -0.187 inches and the analysis results indicated a δ = -0.193 inches (a nominal % difference of only 3.2%), and a very good indication of capturing the correct stiffness of the sandwich in bending. These displacements were in the Y, or vertical direction as well.

The confidence gained in the analysis models, and subsequent correlation with testing will aid in promoting very well qualified systems and more evolved habitat type structures, which will require more rigorous testing, and analysis regimes be conducted. A final set of analyses was conducted for both the inner radius floor beam as well as primary flooring sections utilizing the previous analytical results and approaches.

C. Analysis Models for the Flooring and Inner Radius Floor Support Beam

For the final analytical sequences, both the flooring, and inner radius floor support beam sections, had linear, and non-linear analyses conducted. However, both linear, and non-linear analyses yielded nearly identical results. This is due to the fact that the flooring sections were doubled up back to back, as well as the floor beam web, producing a very stiff design. Unlike a mass optimized structure which would be mandated for space habitats, the applied research effort outlined in this paper represents one step in an evolutionary path to determine numerous factors to leverage this work effort, for direct applications towards flight type qualified hardware for a DSH.

Figure 23 shows the deflection of a representative floor section which is 20 inches long, center to center, between floor supports, 12 inches wide, and is tied down to the lower floor support beams over a bearing area of A= 24in^2 (on the bottom most nodes only). At the ends of the floor strip those planer sections are required to remain planar and vertical. The maximum center span displacement, is denoted by the red contour value and has δ = -0.0026 inches in the Y direction. Analysis shows that the stresses were well within the bounds of any strength limits associated with the sandwich construction and are shown in Fig. 24. However, shown in Fig. 25, is a strain region where core strains reach a nominal $\varepsilon_{vm} \approx 232\mu\varepsilon$, but which occur in the very localized region where the floor section rolls off of the floor beam flange support. It should be noted that the floor strip models themselves are inherently conservative in that the edges of the 12 inch strip have no additional support. In essence, all of the model results reflect the most conservative of responses possible for the sections under study, and verify the large positive margins of safety in the context of strength values.

Shown in Fig. 26 is the specific mesh for the inner radius floor support beam, with the detailed cut outs which allowed for mechanical fastener interface with the support brackets shown in Fig. 6, and the existing bulkhead sections. Figure. 27 is a displacement contour plot of the inner radius floor beam support with an applied pressure load of P = 2.3 psi over the upper flange of the beam. This pressure loading produced a maximum upper flange edge displacement of δ = -0.011 inches (nominal) which is indicated by the red zone in the contour plot. Figure 28 shows the bottom side view of the floor beam support stress response. The figure shows a maximum bearing stress/load riser value of 77psi at the facesheet bracket interface, and a maximum internal core stress = 231psi.

V. Significance of Applied Research Effort and Issues for Future Space Habitats

The applied design, fabrication and research efforts detailed in this report occurred in the context of a 1-g Earth based, analog demonstrator, the HDU-DSH. As such, many of the specific design requirements that need to be addressed for actual space application conditions were not present. In general the sections were overdesigned as a result of both a 1-g loading factor associated with the mass of crew members, possible equipment loadings, unknown random loads, and to mate with existing flooring sections. However, many of the issues addressed in this study are similar to those that will be faced which have design reference missions (DRMs) of LPs, NEOs and/or both Lunar and Martian destinations. Space based systems will necessitate a much greater attention to detail with regards to mass optimization, fabrication, and minimizing any and all non-essential weights associated with all structural sections. One of the principal purposes of this study was to become more familiar with an advanced construction medium, the honeycomb sandwich panel type (which is inherently mass efficient), and delve into the design, fabrication, and experimental and analytical issues which must be addressed for similar sections which will be spaced based.

The development of the novel insert concepts produced in this effort have direct applicability to mechanical fastening techniques for space habitat structures. They are cost effective, lightweight, easily mass produced, and require minimal, or no rework, after production. They are also highly applicable to current aviation industry practices. While standard practice is to confine the sandwich sections to the linear response region, more robust, and hence mass efficient structures, will require that the non-linear material responses outlined in this work be very well understood and accounted for. Additional factors which will need to be accounted for, and which will require additional complexity in terms of design, analysis, fabrication and testing, will be the thermal conditions associated with space habitats and degradation effects associated with the space environment (e.g. micro-meteoroid orbital debris (MMOD)). This paper is a step in the direction of addressing the much greater complexities, and the numerous issues, which will face state of the art structural implementations for space habitats.

VI. Conclusions

Design constraints, and requirements for micro-gravity environments, and deep space applications will be much more rigorous and resource critical than terrestrial prototypes. Sizing for microgravity, and launch loads, will differ substantially from those in a terrestrial gravity condition as well, however, the types of structural construction, and many of the same considerations, will be relevant. The honeycomb composite type construction, detailed in this report, has gained general acceptance within the aviation industry and constitutes an effective structural option for space habitats as well. Similar issues faced in general aviation applications, i.e. inserts, mechanical fastening approaches, adhesive systems, core outs and close out sections, and hardware attachment points, can be evolved for space relevant flight type applications. General fabrication methods which are cost effective, may not be suitable for mass optimized systems which will require higher fidelity design and analysis.

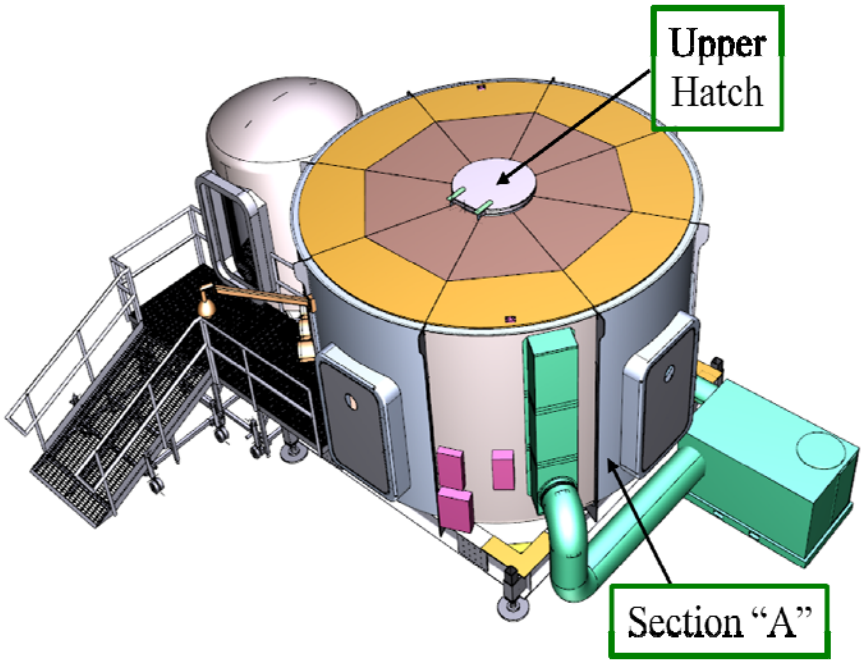

Figure 1. HDU-DSH External view.

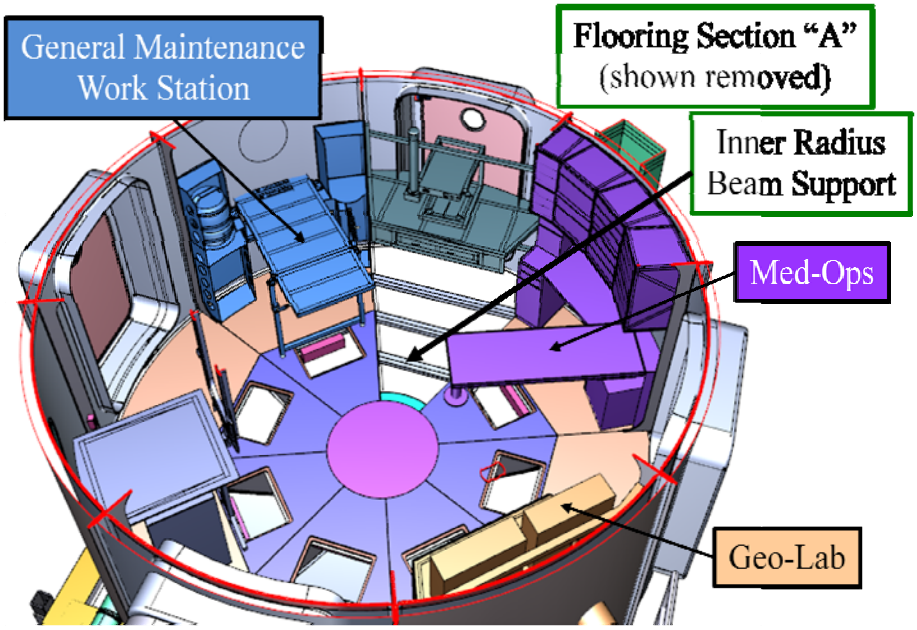

Figure 2. Sectional view of the HDU-DSH with flooring section "A" removed for clarity.

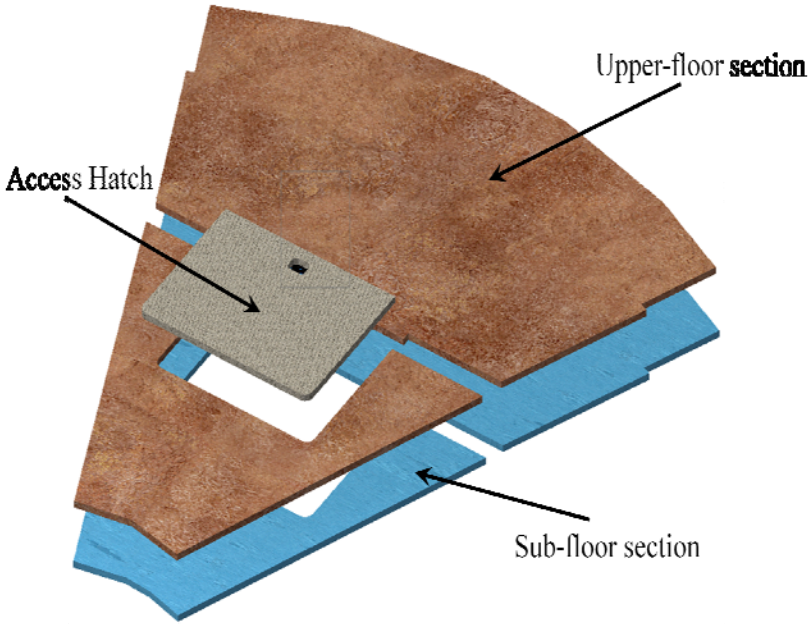

Figure 3. Exploded view of flooring section A components.

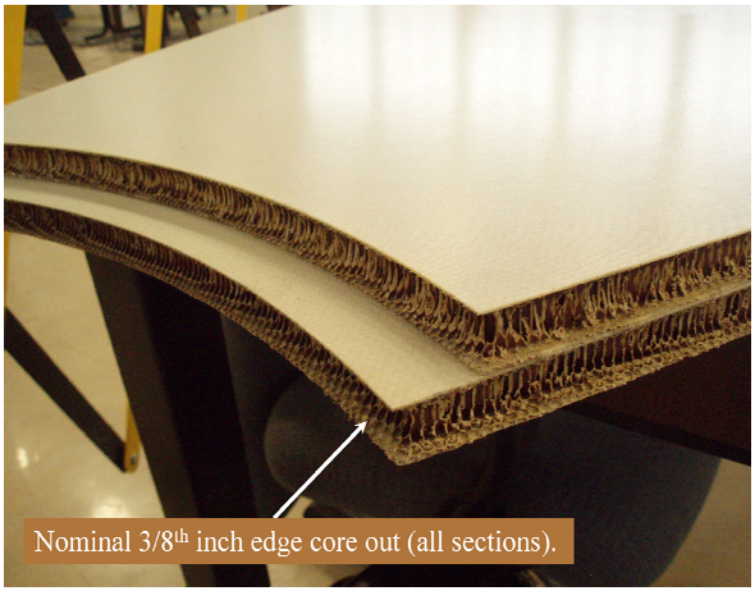

4a. Primary flooring edge core out.

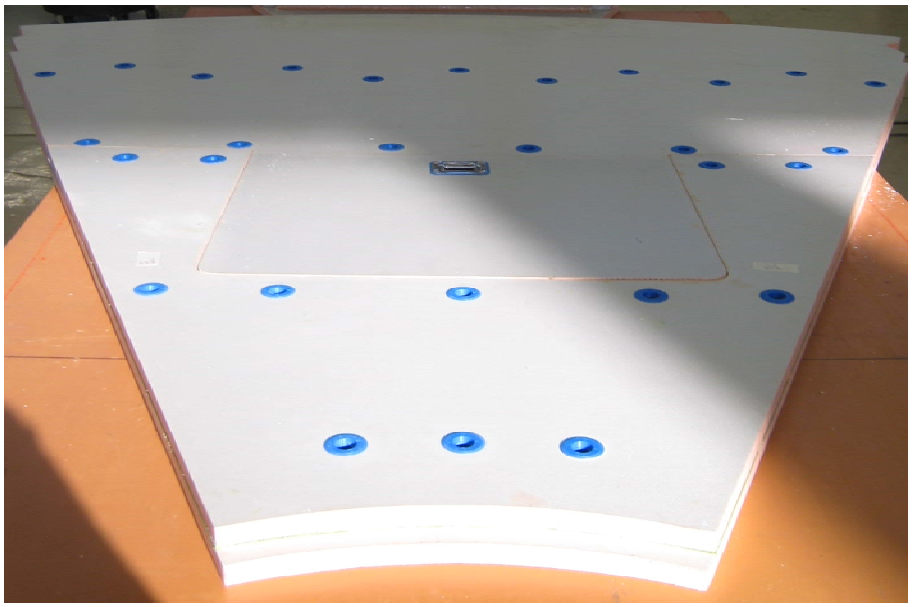

4b. Finished panel ready for shipment.

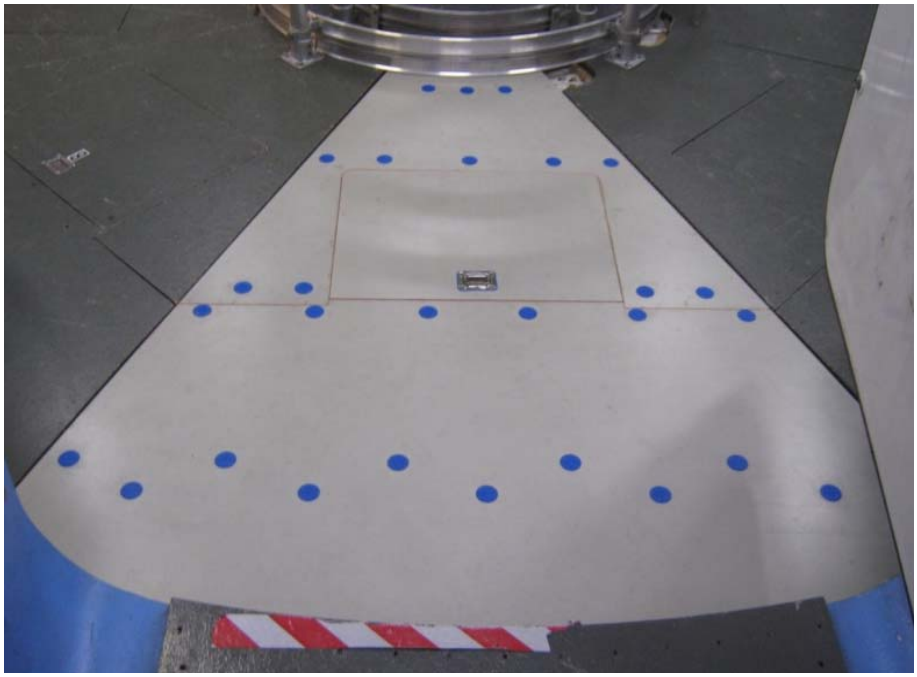

4c. Installed evolved flooring panel within the HDU-DSH.

Figure 4. Edge core out. final construction with inserts, and as installed.

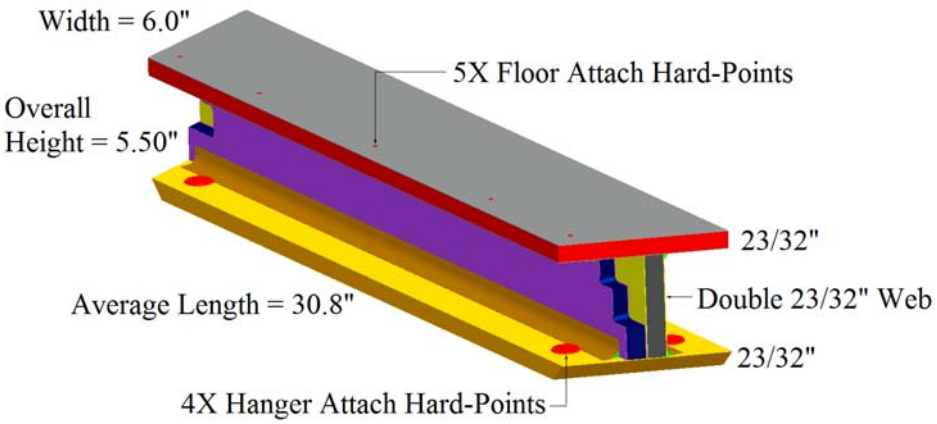

5a. Orthogonal design sketch of floor beam with details.

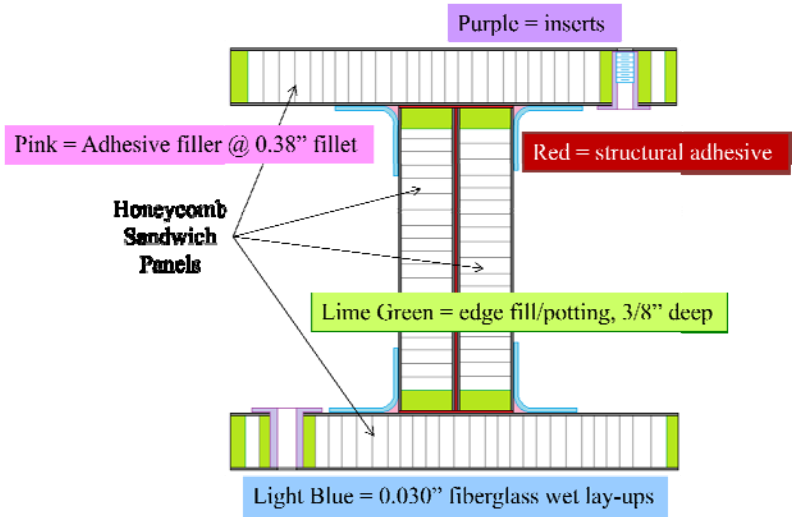

5b. Specific construction details of evolved floor beam.

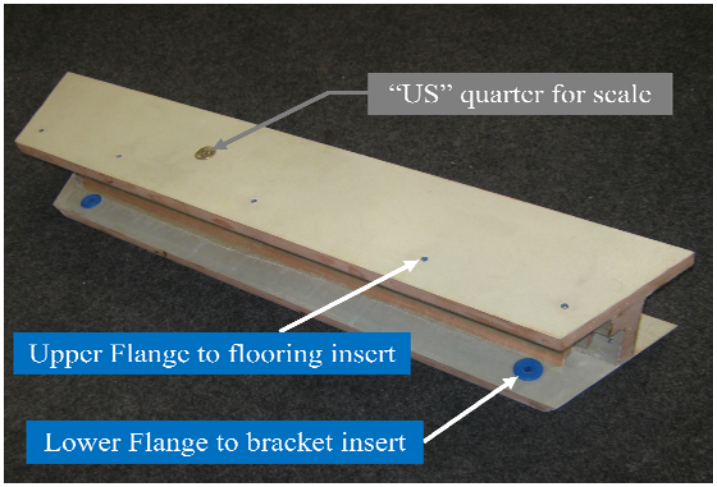

5c. Matched drilled inner radius beam with inserts ready for installation.

Figure 5. Specifics of the inner radius beam floor support.

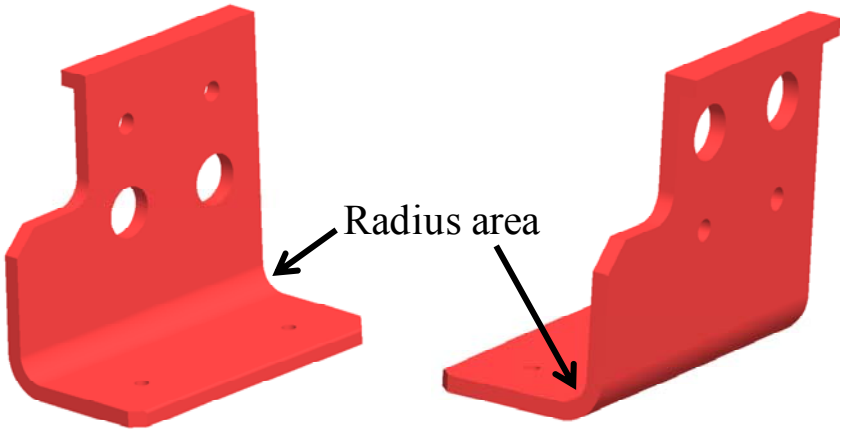

Figure 6. Bulkhead bracket pair for the floor beam support.

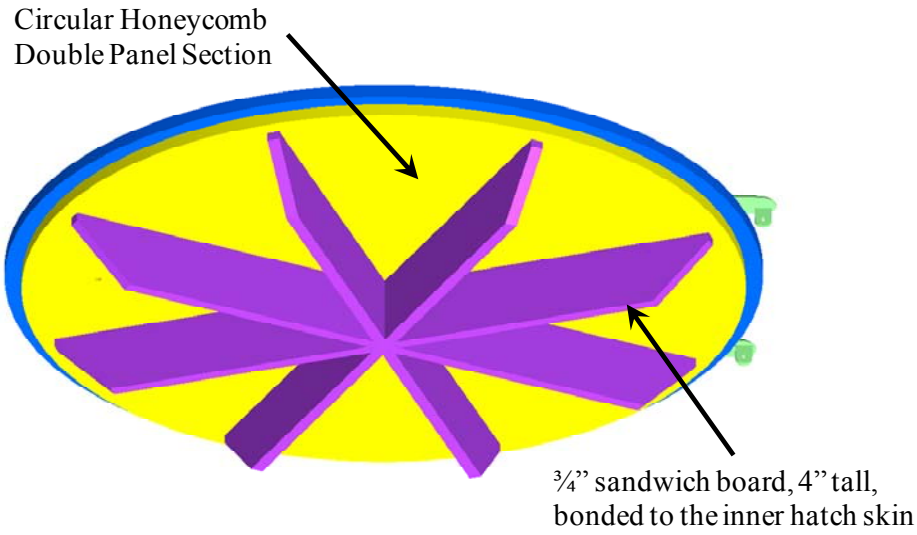

Figure 7. Initial upper hatch structural concept.

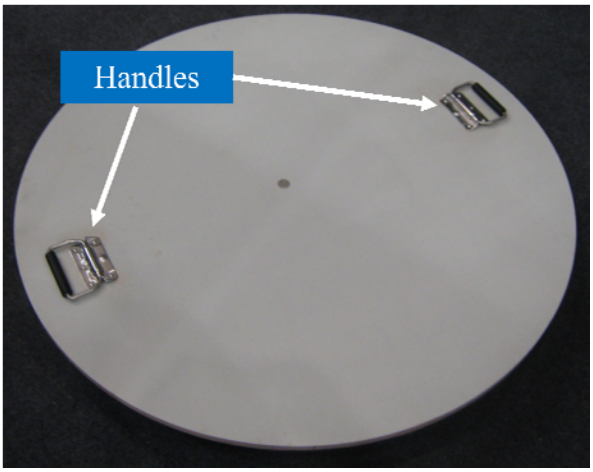

8a. Upper hatch concept #1 upper surface.

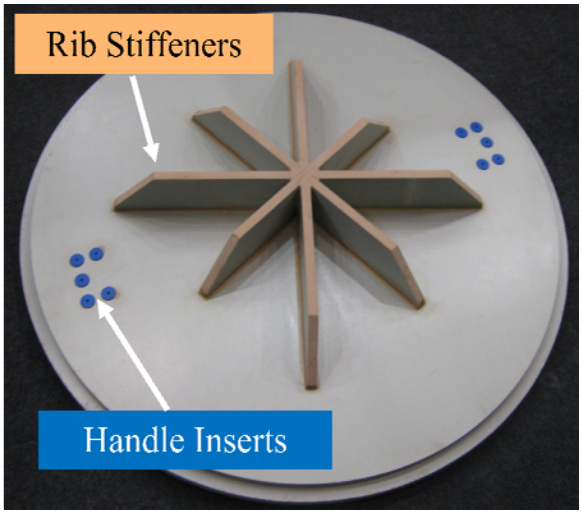

8b. Upper hatch concept #1 lower surface.

8c. Handle details on hatch concept #1.

Figure 8. Hatch concept #1 hardware specifics.

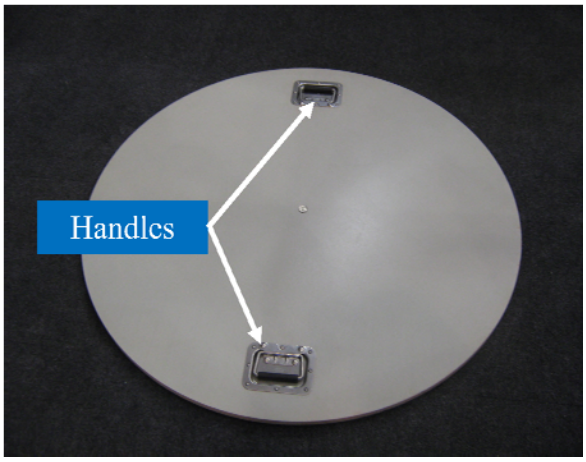

9a. Hatch concept #2 upper surface.

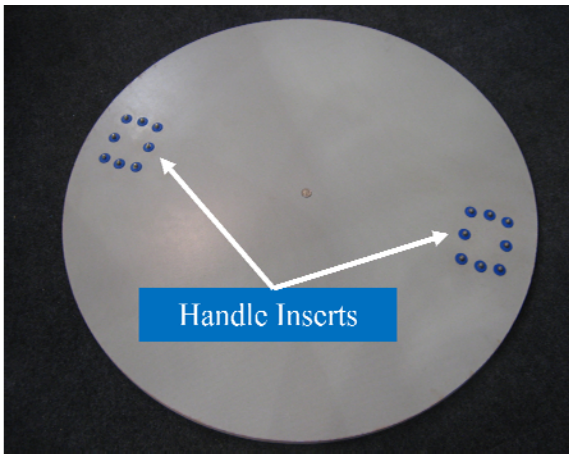

9b. Hatch concept #2 lower surface.

9c. Hatch concept #2 handle.

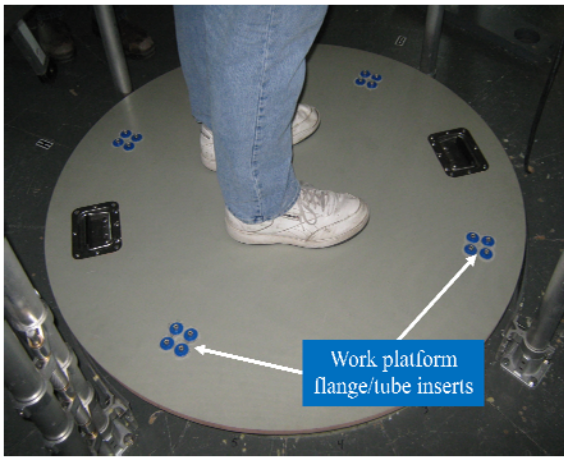

9d. Installed onto work platform.

9e. Flange leg interface section.

Figure 9. Hatch concept #2 hardware specifics.

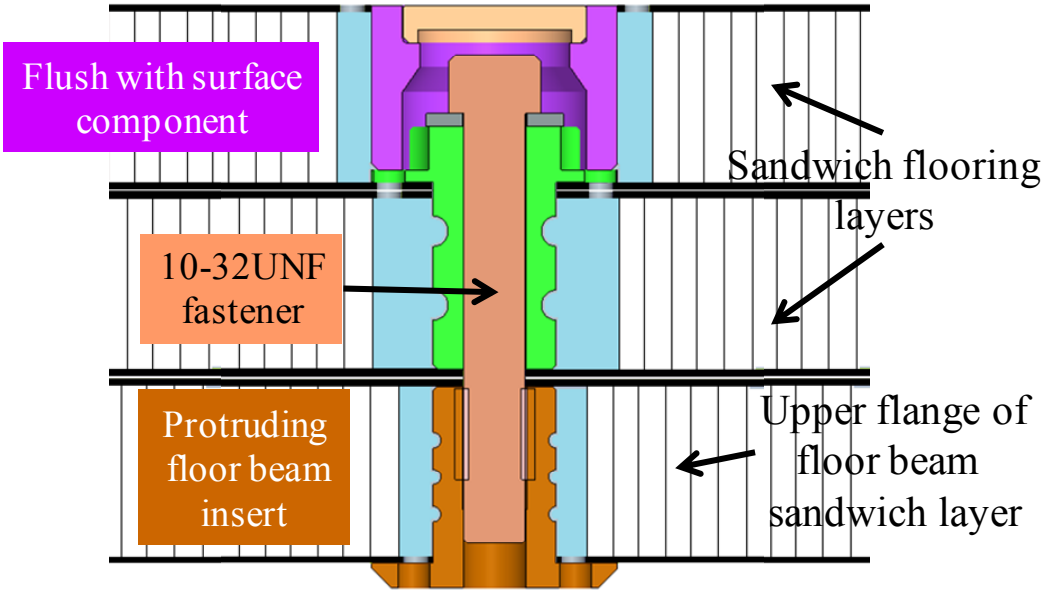

10a. Flush with surface insert concept details.

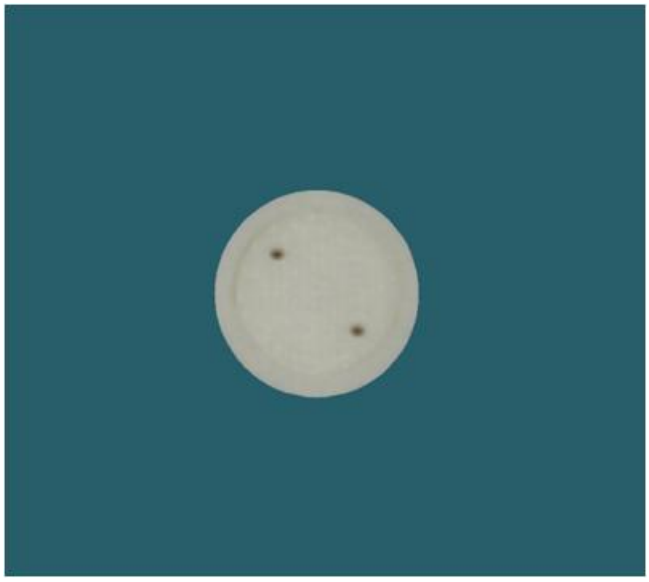

10b. Installed flush with surface insert.

10. Flush with surface insert concept.

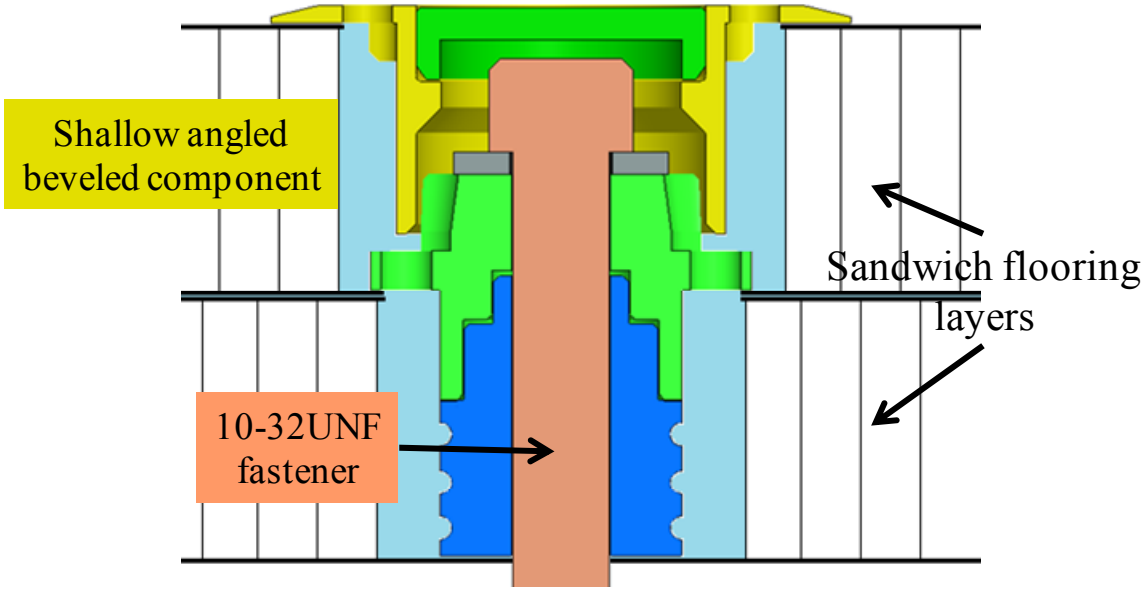

11a. Shallow angled beveled edge insert concept details.

11b. Installed shallow angled beveled edge insert.

11. Shallow angled beveled edge insert concept.

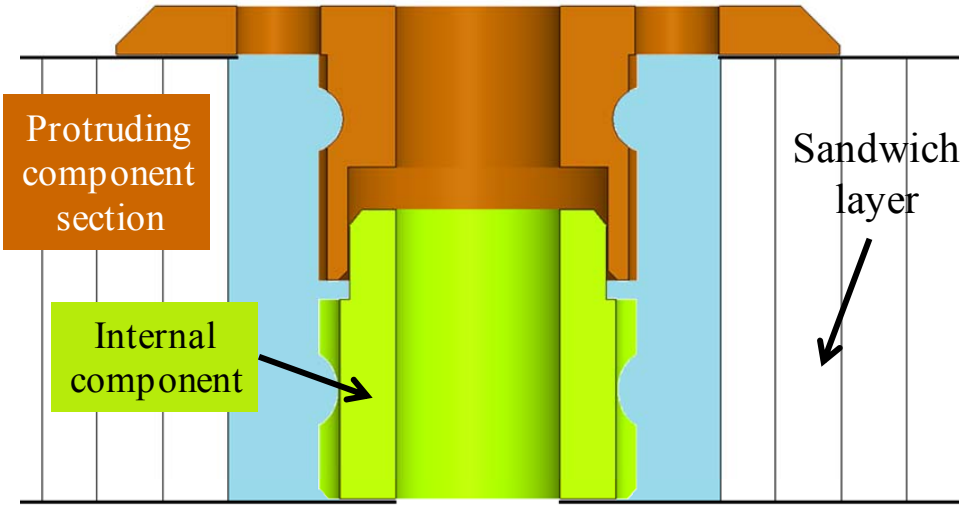

12a. Proud protruding insert concept details.

12b. Installed proud protruding insert.

12. Proud protruding insert concept.

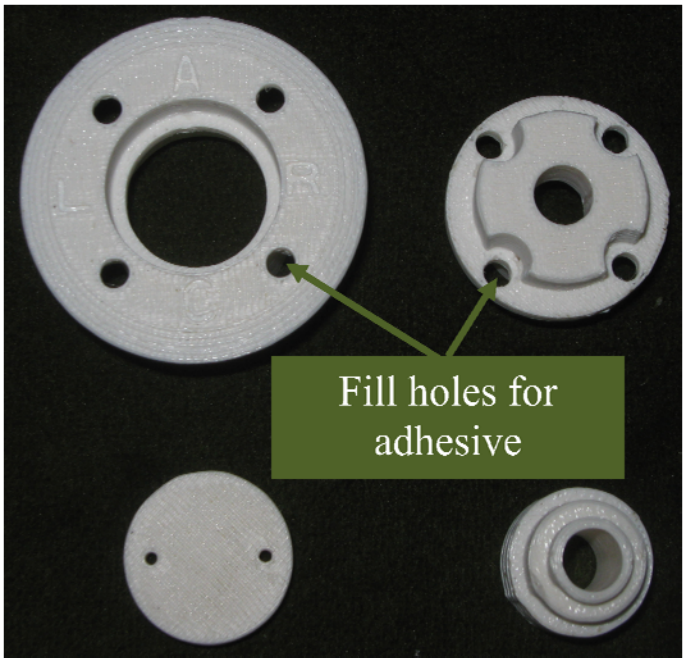

13a. Multi-part components.

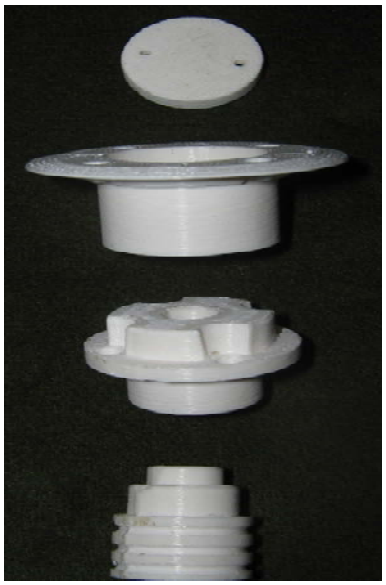

13b. Component assembly.

13c. Assembled initial insert concept.

13. Multi-part initial floor insert concept.

14a. Components of the GitD Concept.

14b. Final assembled GitD.

14. Multi-part initial glow in the dark floor insert concept #2.

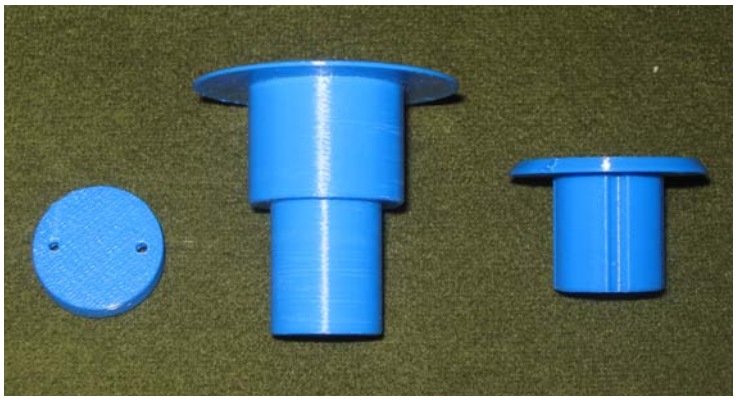

15a. Flooring insert cap, flooring insert, and FB insert.

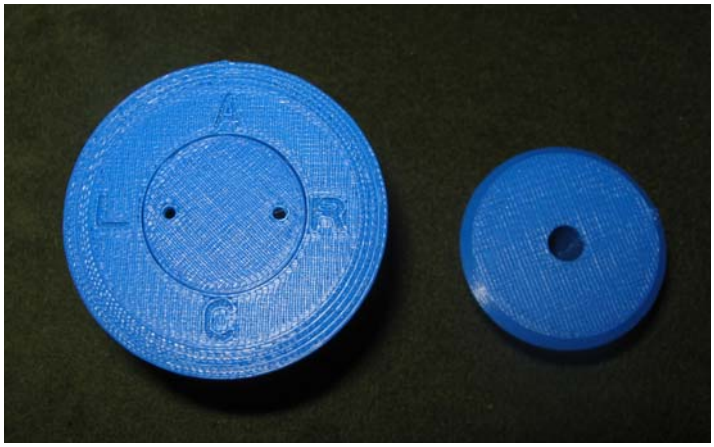

15b. Top view of final inserts.

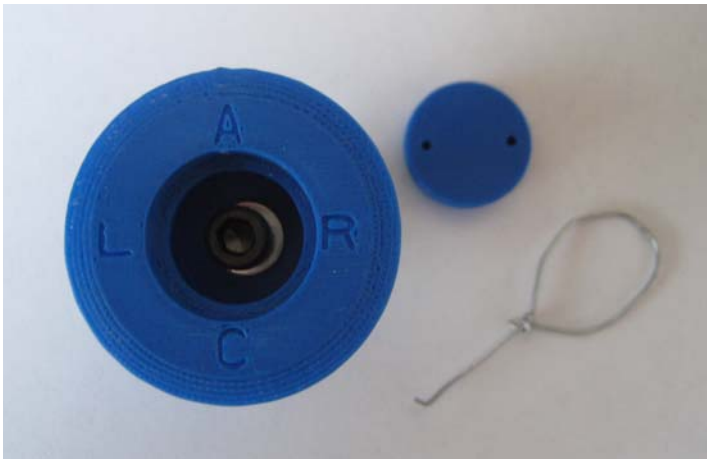

15c. Final implemented floor inset concept showing 10-32UNF fastener, as well as cap removal tool (aka paper clip).

15. Final flooring and floor beam insert concepts as installed.

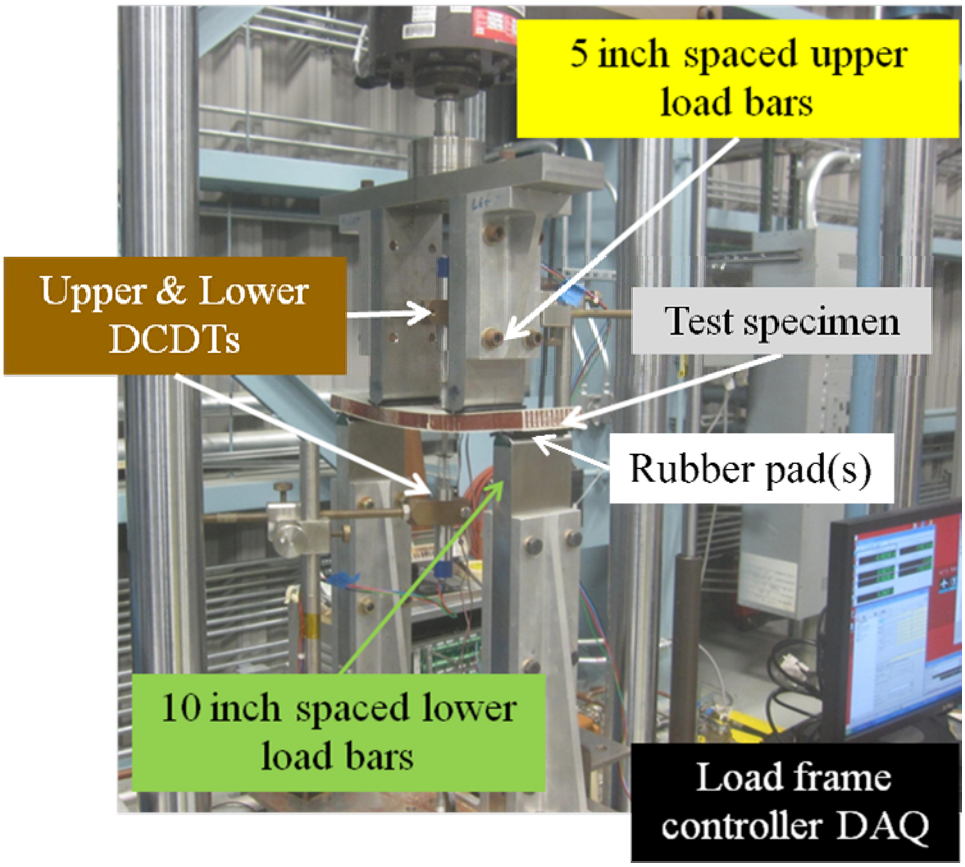

Figure 16. 4-point bending test fixture.

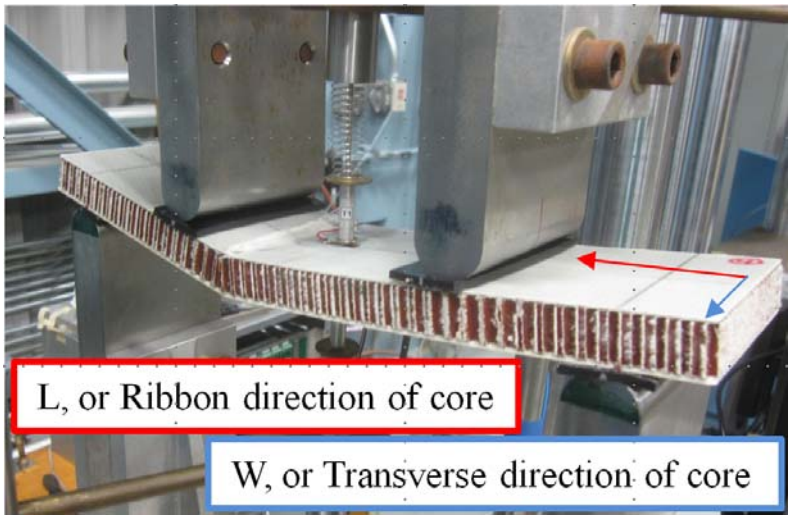

Figure 17. Typical ultimate compressive stress failure on upper facesheet.

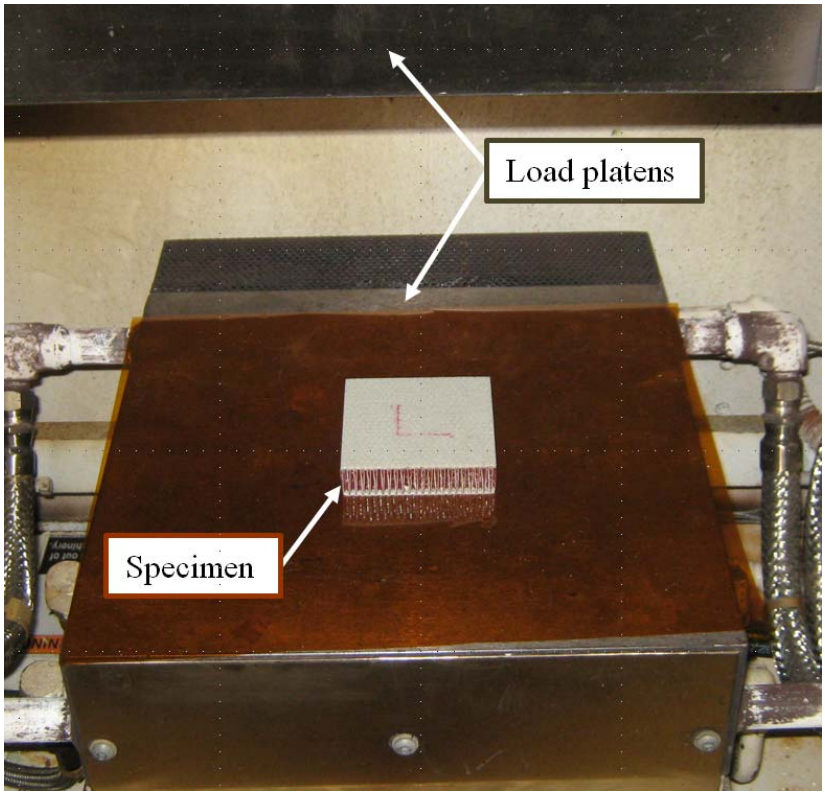

Figure 18. Core crush test set-up.

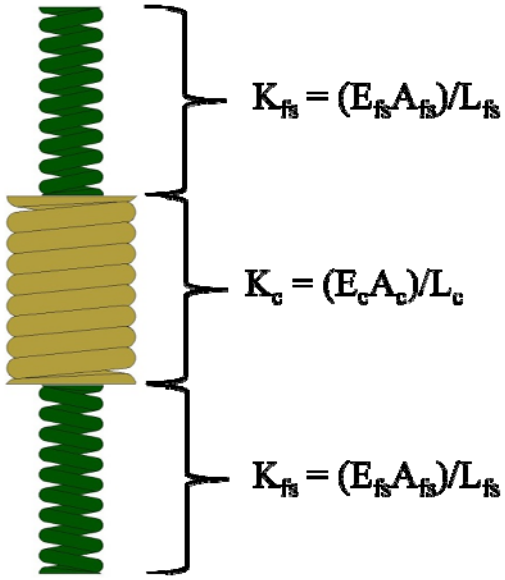

Figure 19. Springs in series stiffness components.

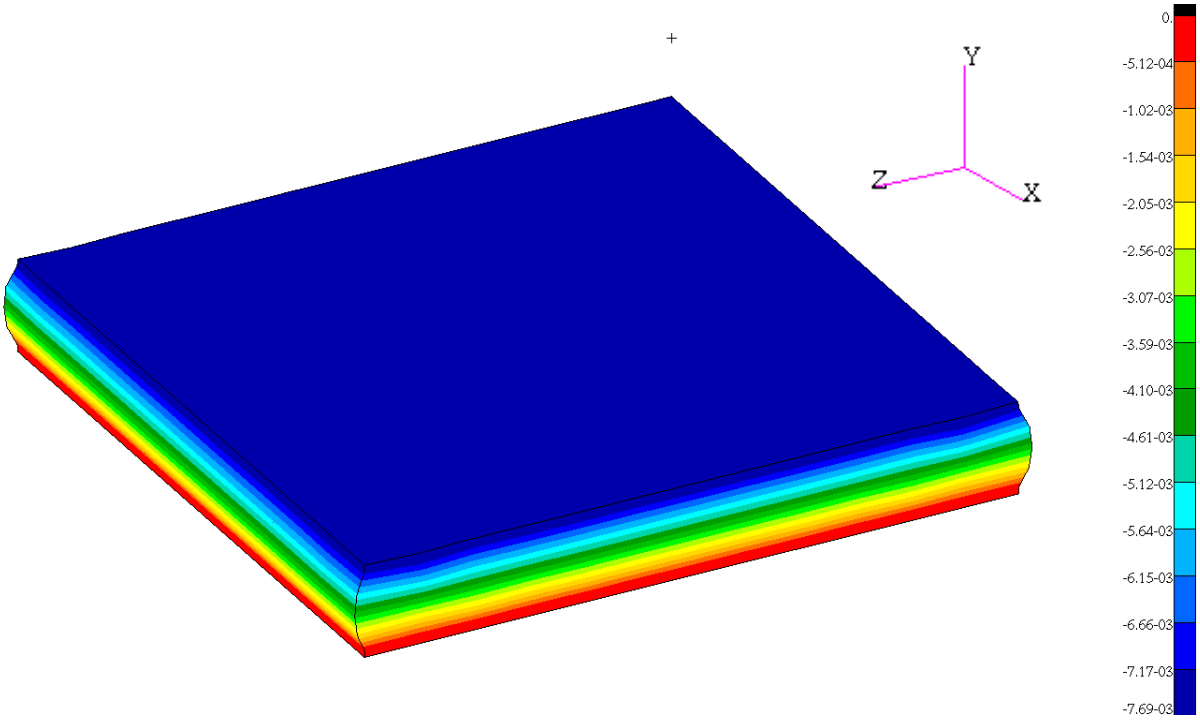

Figure 20. Core crush patch test uniform pressure loading, Y direction displacements, inches.

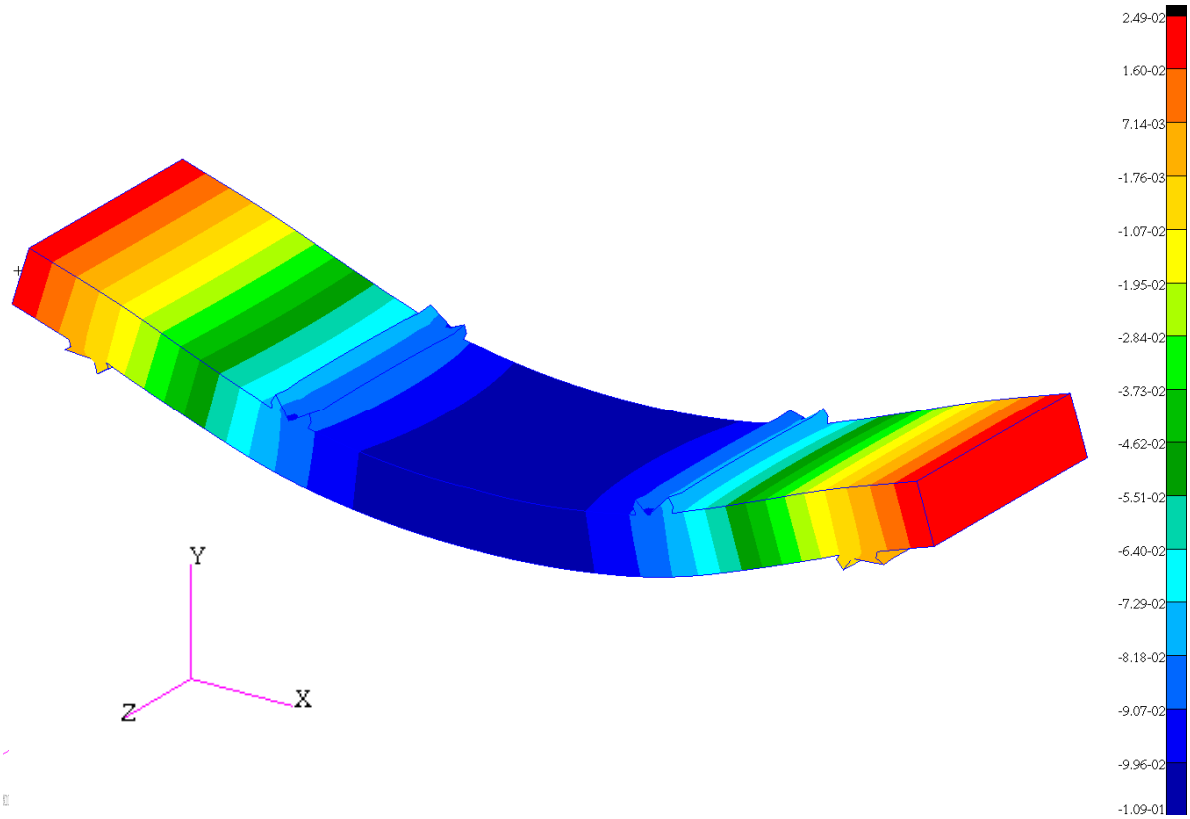

Figure 21. Mid-span deflection for the 4-point bending linear analysis, Y direction, inches.

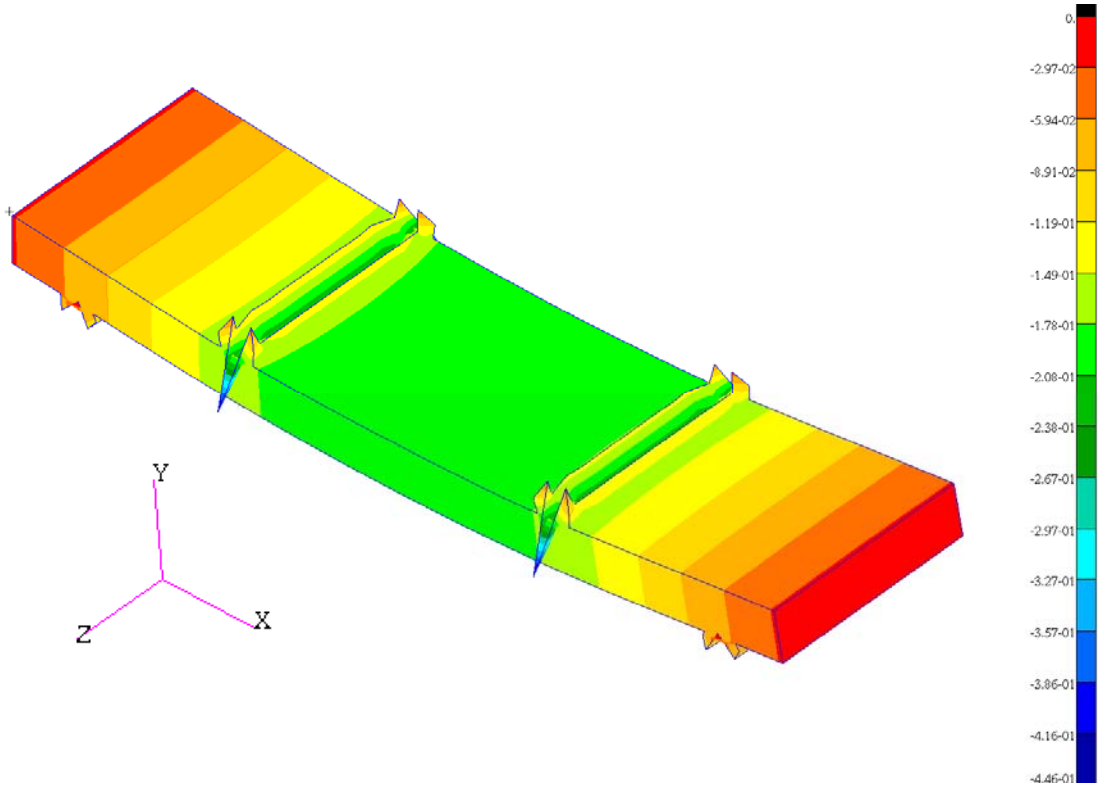

Figure 22. Displacement response of the 4-point bending non-linear analysis, Y direction, inches.

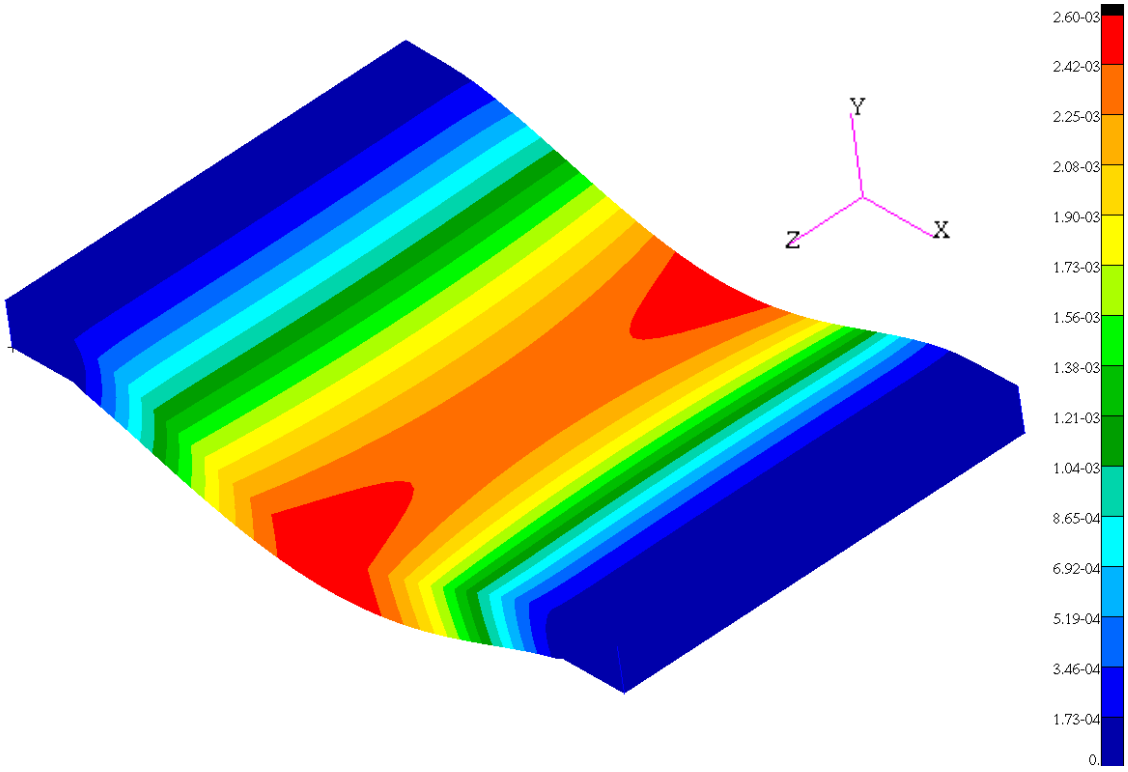

Figure 23. Midspan deflection of floor panel section, Y direction, inches.

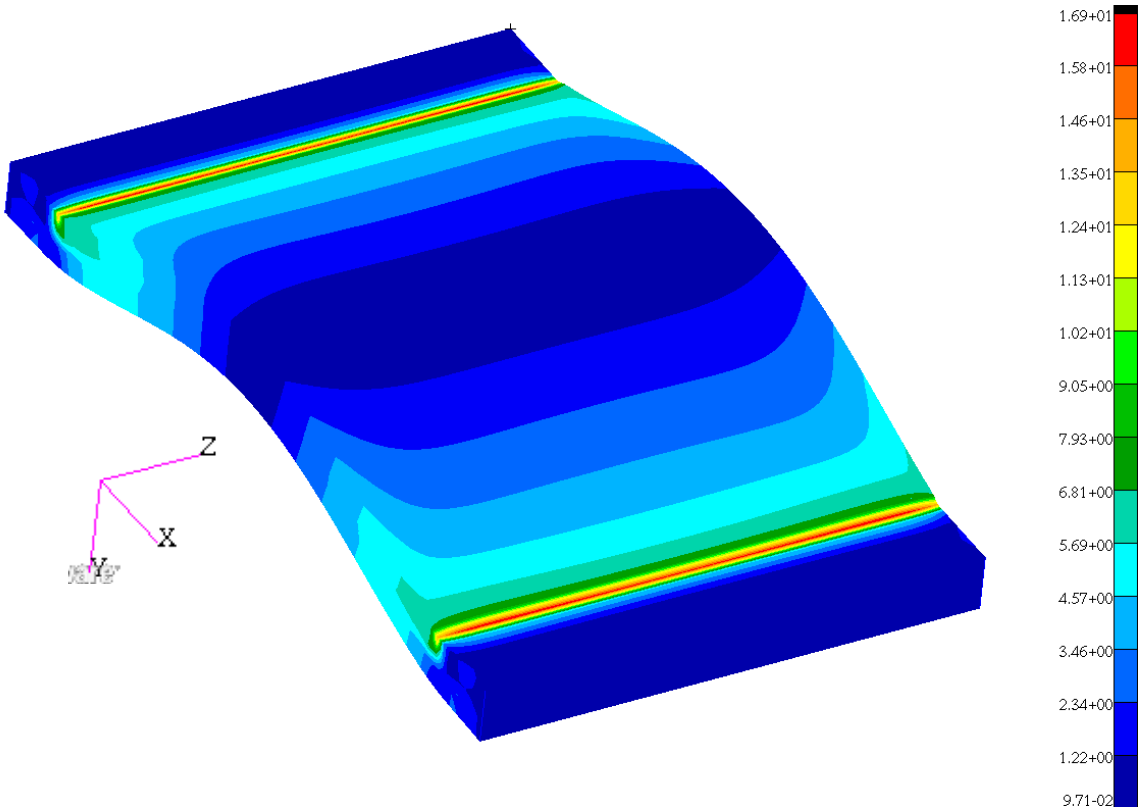

Figure 24. Von-Mises stress response of flooring, psi.

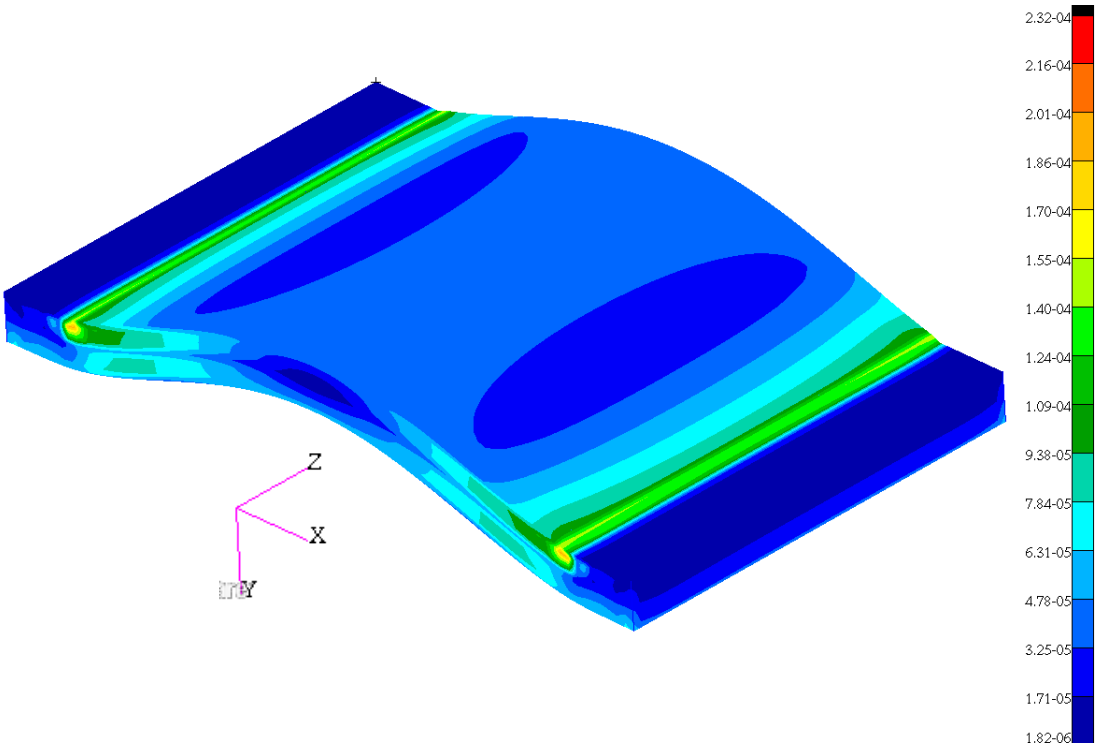

Figure 25. Localized core strains near support roll off location, Von-mises, micro-strain.

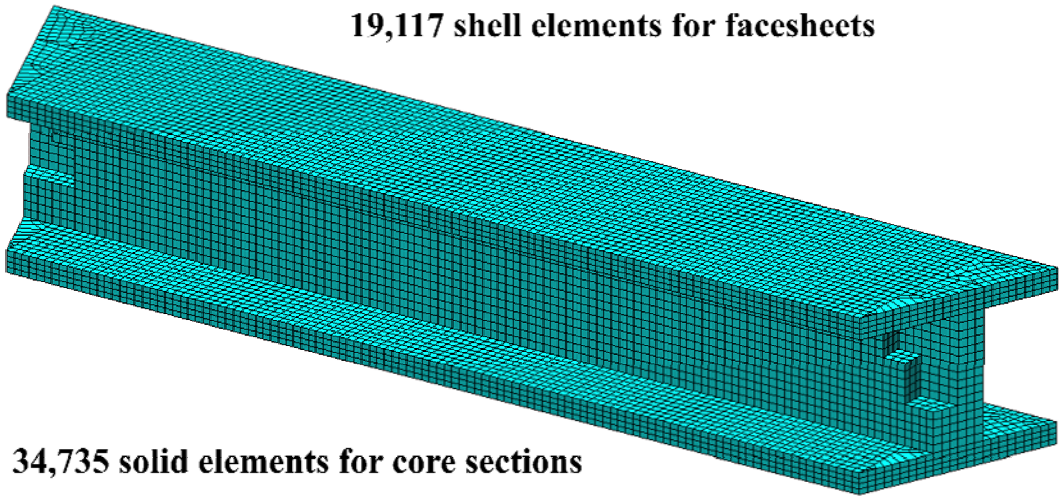

Figure 26. Finite element mesh specifics for the inner radius floor support beam.

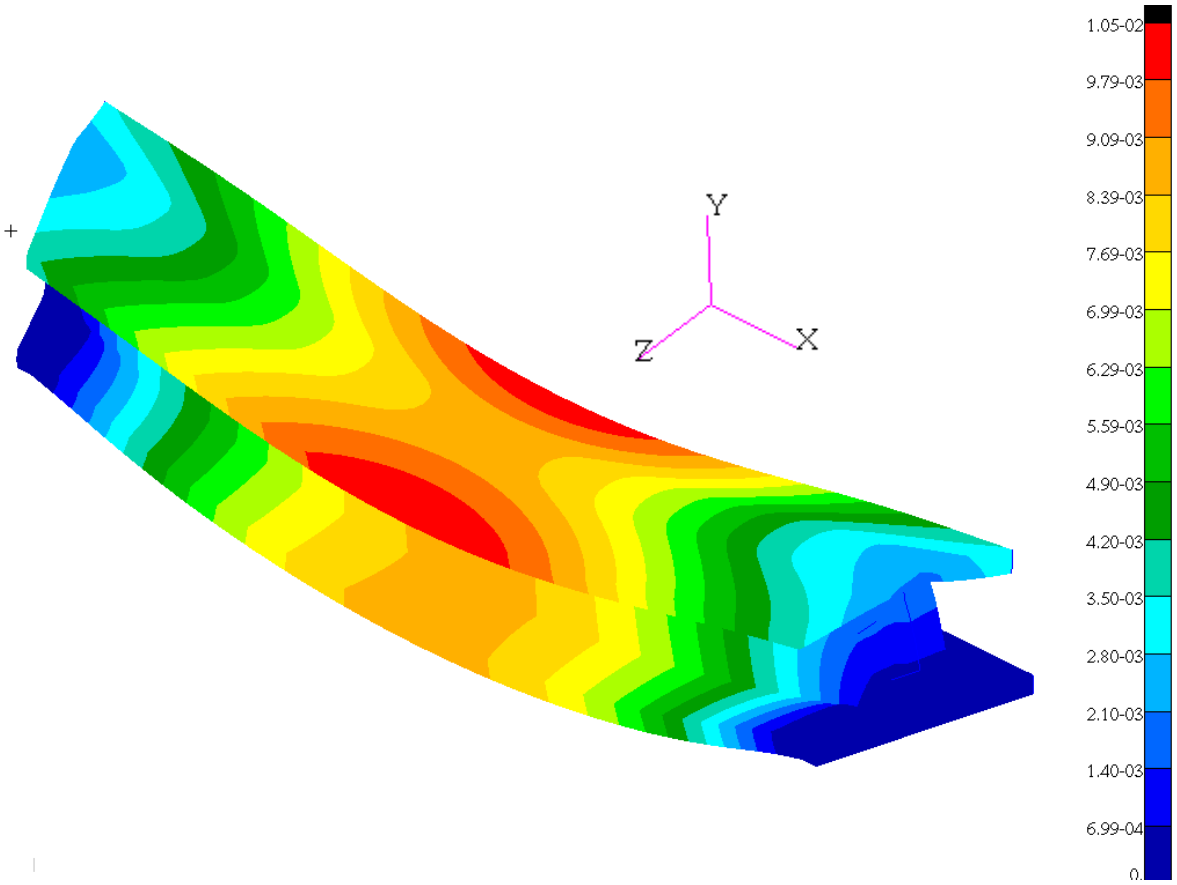

Figure 27. Displacement response of the inner radius floor support beam, Y direction, inches.

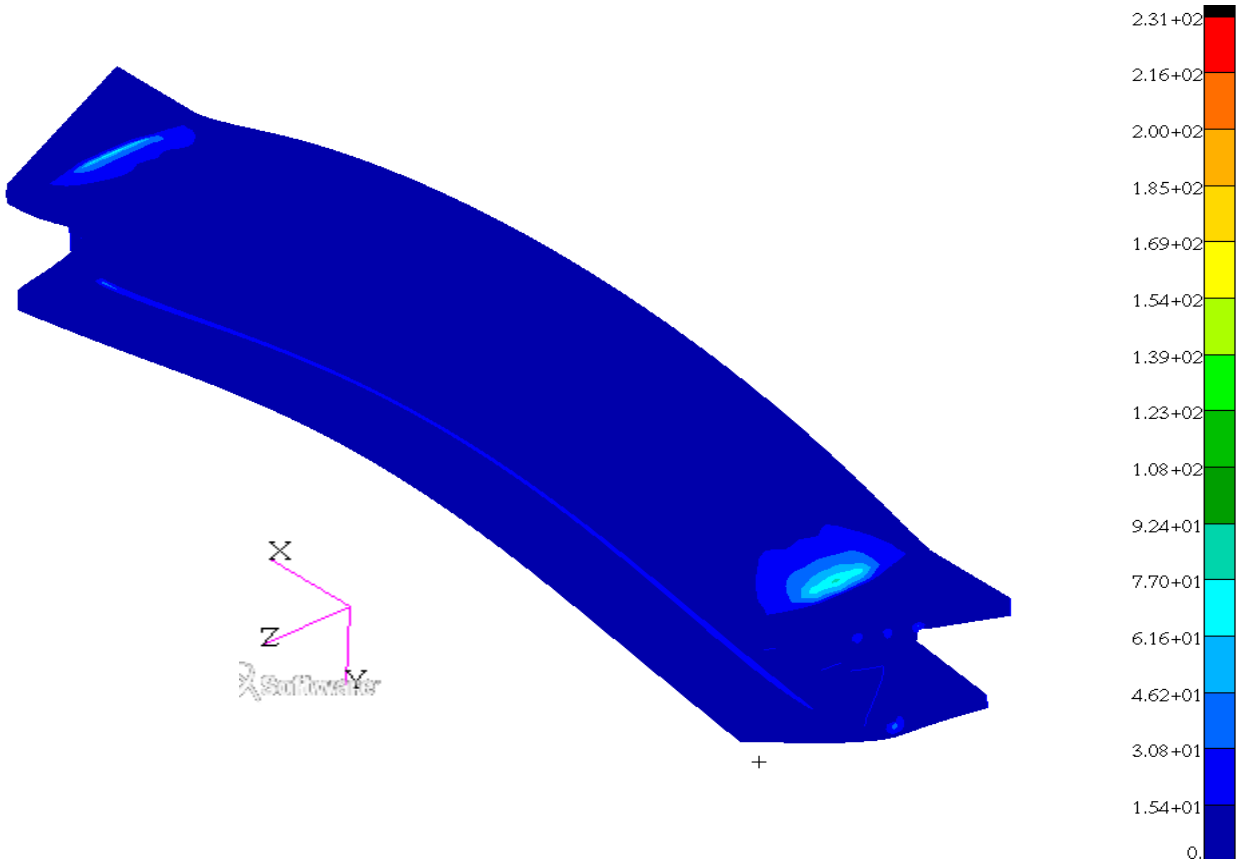

Figure 28. Stress response of the inner radius floor support beam, Von-mises, psi.

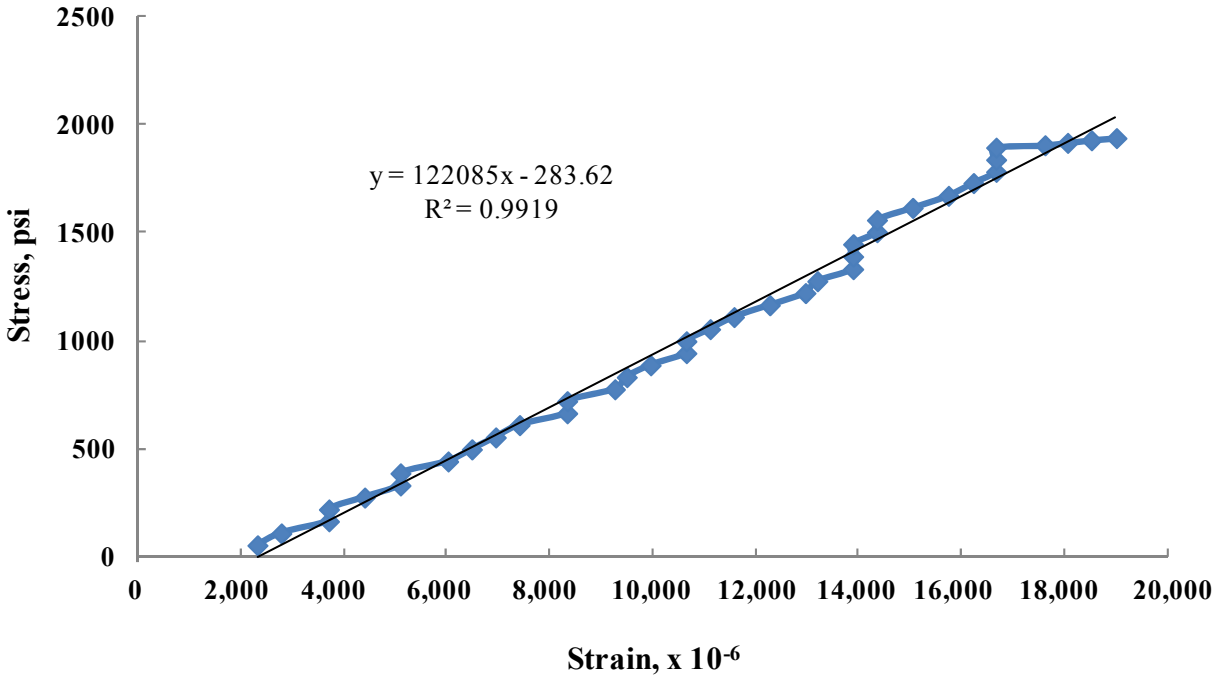

Figure 29. Stress vs. Strain for core crush test.

Table 1. Compiled Ultimate Modulus and Ultimate Facesheet Stresses

Average (psi)	Ultimate Modulus-L	Ultimate Modulus-W
Tension	*2390120*	2604576
Compression	2450550	2500905
Ultimate Strength	+-31000	+-25228

Table 2 Specific Values for the Nomex Honeycomb Core Section with Lc = 0.500 inches

Properties of Gillfab HD - Non-Metallic Honeycomb
Based on .500" thick slice unless stated otherwise
Typical average property values

PROPERTY	UNIT (Eng./Metric)	1/8 CELL (±10%)		3/16 CELL (±10%)
Nominal Density		8.0 PCF	9.0 PCF	6.0 PCF
Cell Size	in (mm)	0.134 (3.4)	0.135 (3.4)	0.196 (5)
Bare Compression	PSI (N/mm²)	1,665(11.48)	2,031 (14.00)	94 (6.85)
Stabilized Compression	PSI (N/mm²)	1,750(12.07)	2,133 (14.71)	1,120 (7.72)
Shear - L Direction Ultimate Load Modulus	 PSI (N/mm²) PSI (N/mm²)	 548 (3.778) 18,610(128.3)	 564 (3.889) 20,510(14.4)	 590 (4.068) 17,000(117.2)
Shear - W Direction Ultimate Load Modulus	 PSI (N/mm²) PSI (N/mm²)	 397 (2.737) 10,370(71.5)	 423(2.917) 12,110 (83.5)	 388 (2.675) 9,900 (68.3)
Water Migration	Number of contiguous cells	1.00	1.47	1.08
Flammability -60 Second Vertical Self-Extinguishing Time Burn Length Drip Extinguishing Time	 second inch (mm) second	 1.3 2.9 (74) 0	 0.1 0.5 (13) 0	 1.9 1.6 (41) 0

Appendix A[12-14]: Pro-E Flooring Stress Analysis Based Upon $\rho_c = 3$ lbs/ft^3

The flooring is analyzed in this section as a simply supported beam. The flooring section of Section A is shown below:

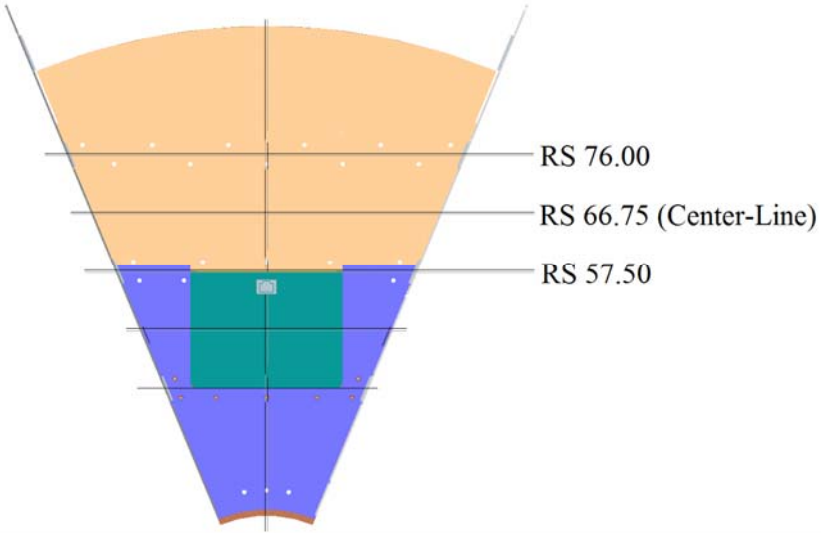

Figure 30. Initial flooring analysis beam spacings.

In the above snapshot the largest unsupported section is assumed to be between Radial Station (RS) 57.50 and RS 76.00. This section is simplified as a rectangle as shown below for the MC Gill analysis:

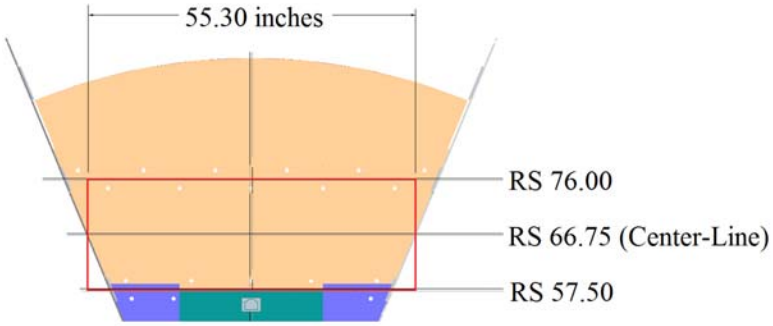

Figure 31. Initial rectangular double floor stack analysis.

In the above sketch the floor section is 55.3 inches long and 18.5 inches wide. Therefore,

a = span = 55.3 inches
b = width = 18.5 inches

The flooring is comprised of two layers of sandwich board. This sandwich board has 0.030 inch thick fiberglass face sheets and a 1/8 inch cell size, honeycomb core (a.k.a. Nomex) with a density of 3.0 pounds per cubic foot. For analysis purposes a CAD model is used to find the area of inertia for the face sheets. The model is shown below:

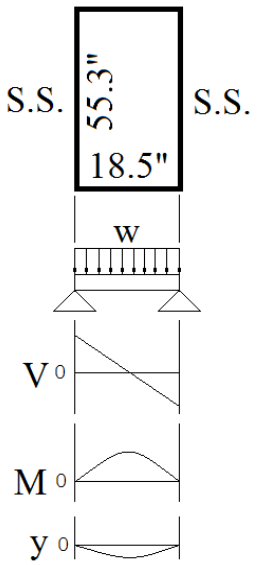

For a 50lbs/ft^2 floor loading the total load is

$$F_{Floor} = (50psf)(55.3in)(18.5in)(1/144)$$
$$F_{Floor} = (50psf)(7.1\ s.f.)$$
$$F_{Floor} = 355\ \text{lbs.}$$

This relates to a beam loading of,

$$w = \frac{355\ \text{lbs.}}{18.5\ \text{in}}$$
$$w = 19.2\ \text{lbs./in.}$$

And, the maximum moment created is,

Figure 32. Displacement, bending and shear response of initial analysis.

$$M_{max} = \frac{w\,x}{2}(1-x) = \frac{w\left(\frac{1}{2}\right)}{2}\left(1-\frac{1}{2}\right)$$
$$M_{max} = \frac{(19.2)(9.25)}{2}(18.5-9.25) = \frac{(19.2)(9.25)^2}{2}$$
$$M_{max} = 821\ \ in.-lbs.$$

Shown below is the CAD model of the skin model with a cross-section cut down the middle:

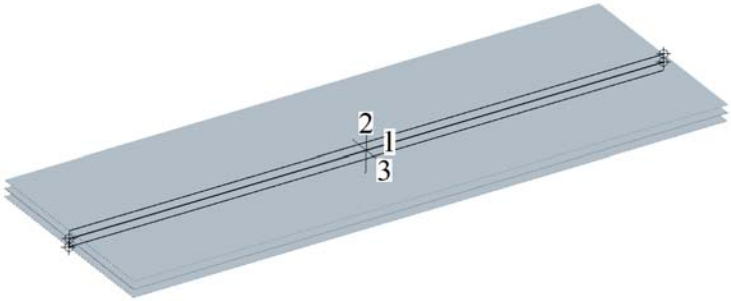

Figure 33. Pro-E CAD model of initial analysis.

From the Pro-Engineer CAD model of the skins, the area moment of inertia into the page (the 55.3 inch direction) of the above diagram is,

From the above data, $z = I/c = 2.39\ in^3$, Therefore, the maximum stress is,

$$\sigma = \frac{Mc}{I} = \frac{M}{z} = \frac{821}{2.39}$$
$$\sigma = 343\ psi$$

From the above data, $z = I/c = 2.39$ in^3. Therefore, the maximum stress is,

$$\sigma = \frac{M\,c}{I} = \frac{M}{z} = \frac{821}{2.39}$$

$$\sigma = 343 \text{ psi}$$

Acknowledgments

The authors would like to acknowledge the following individuals and organizations:

Richard Chattin, Sean Britton, Hou Luong & Janice Smith of the Materials Experiments Branch at NASA LaRC, additionally Quinton Duncan & Kathy Duvol of the Structures Experiments Branch. Additionally, thanks are given to Dr. Scott Howe for the use of his interactive HDU-DSH prototype model which produced the first two figures in this publication. Also, our friends and colleagues at the Johnson Space Center, with whom this work was jointly conducted and implemented. An additional thanks goes out to Amy Brewer, assigned to the Structural Mechanics & Concepts Branch for her superlative testing support.

References

[1] Kennedy, K.J. and Capps, Stephen D: *Designing Space Habitation.* Presented at the Space 2000 Conference, Long Beach, California, Sept. 19-20.

[2]Dorsey, J.T., Wu, K.C. and Russ Smith: *Structural Definition and Mass Estimation of Lunar Surface Habitats for the Lunar Architecture Team Phase 2 (LAT-2) Study.* Presented at the ASCE Earth & Space Conference, Long Beach, California, 3-5 March 2008.

[3]Gill, T.R., Merbiz, J.C., et al..: *Habitat Demonstration Unit Pressurized Excursion Module Systems Integration Strategy.* International Conference on Environmental Systems, Portland, Oregon, 18-21 July 2011.

[4]Kennedy, K.J., Gill, T.R., et al..: *Habitat Demonstration Unit Project - Deep Space Habitat Overview.* Proceedings of the 4st International Conference on Environmental Systems (ICES 2011); Portland, Oregon, 18-21 July 2011.

[5]MacLeod, J. (compilation): Instructions for the Fabrication, Installation, and Repair of M.C. Gill Corp. Cargo Liners and Decompression Panels in Airbus Aircraft.

[6]M.C. Gill Corporation, Report No. MCG IRM 9701, Revision G: Instructions for the Fabrication, Installation, and Repair of M.C. Gill Corp. Cargo Liners and Decompression Panels in Airbus Aircraft.

[7]ASTM D7249 / D7249M - 06 Standard Test Method for Facing Properties of Sandwich Constructions by Long Beam Flexure.

[8]Petras, A., Sutcliffe, M.P.F., "Failure mode maps for honeycomb sandwich panels," Composite Structures 44 (1999) 237-252, Cambridge University, Engineering Department, Trumpington Street, Cambridge CB2 1PZ, UK.

[9]MD/MSC Nastran 2010 Quick Reference Guide, DOC9467, 20 July 2010. MSC Corporation,.

[10]PATRAN 2010.2.3 Release Guide, DOC9752, 23 Feb 2011. MSC Corporation.

[11]Niu, Michael, C.Y., *Airframe Structural Design*, 2nd ed., Hong Kong Conmilit Press Ltd., Hong Kong, 1999, Chaps. 10.

[12]Langford, W.M.: HDU-2 Flooring Analysis, NASA, LaRC, July 2011.

[13]Pro Engineer, Wildfire 4.0, Date Code M160 Copyright 2008 Parametric Technology Corporation.

[14]Mc Gill Publication (Reference: www.mcgillcorp.com, "MC-GILL-3_97_Summer.pdf", Volume 34, Summer 1997, Number 3).